European Journal of Medicinal Chemistry 122 (2016) 27–42

Contents lists available at ScienceDirect

European Journal of Medicinal Chemistry

journal homepage: http://www.elsevier.com/locate/ejmech

Research paper

Dopaminergic isoquinolines with hexahydrocyclopenta[*ij*]-isoquinolines as D_2-like selective ligands

Javier Párraga [a], Sebastián A. Andujar [b], Sebastián Rojas [b], Lucas J. Gutierrez [b], Noureddine El Aouad [c], M. Jesús Sanz [d, e], Ricardo D. Enriz [b], Nuria Cabedo [d, *], Diego Cortes [a, **]

[a] Departamento de Farmacología, Laboratorio de Farmacoquímica, Facultad de Farmacia, Universidad de Valencia, 46100, Burjassot, Valencia, Spain
[b] Facultad de Química, Bioquímica y Farmacia, Universidad Nacional de San Luis-IMIBIO-SL, Chacabuco 915, 5700, San Luis, Argentina
[c] Campus Universitaire Ait Melloul, Université Ibn-Zohr, Agadir, Morocco
[d] Institute of Health Research-INCLIVA, University Clinic Hospital of Valencia, 46010, Valencia, Spain
[e] Departamento de Farmacología, Facultad de Medicina, Universidad de Valencia, 46010, Valencia, Spain

ARTICLE INFO

Article history:
Received 14 March 2016
Received in revised form
7 June 2016
Accepted 8 June 2016
Available online 10 June 2016

Keywords:
Tetrahydroisoquinolines
Hexahydrocyclopentaisoquinolines
Dopaminergic
Structure-activity relationships
Cytotoxicity
Molecular modeling

ABSTRACT

Dopamine receptors (DR) ligands are potential drug candidates for treating neurological disorders including schizophrenia or Parkinson's disease. Three series of isoquinolines: (*E*)-1-styryl-1,2,3,4-tetrahydroisoquinolines (series 1), 7-phenyl-1,2,3,7,8,8a-hexahydrocyclopenta[*ij*]-IQs (HCPIQs) (series 2) and (*E*)-1-(prop-1-en-1-yl)-1,2,3,4- tetrahydroisoquinolines (series 3), were prepared to determine their affinity for both D_1 and D_2-like DR. The effect of different substituents on the nitrogen atom (methyl or allyl), the dioxygenated function (methoxyl or catechol), the substituent at the β-position of the THIQ skeleton, and the presence or absence of the cyclopentane motif, were studied. We observed that the most active compounds in the three series (**2c**, **2e**, **3a**, **3c**, **3e**, **5c** and **5e**) possessed a high affinity for D_2-like DR and these remarkable features: a catechol group in the IQ-ring and the N-substitution (methyl or allyl). The series showed the following trend to D_2-RD affinity: HCPIQs > 1-styryl > 1-propenyl. Therefore, the substituent at the β-position of the THIQ and the cyclopentane ring also modulated this affinity. Among these dopaminergic isoquinolines, HCPIQs stood out for unexpected selectivity to D_2-DR since the Ki D_1/D_2 ratio reached values of 2465, 1010 and 382 for compounds **3a**, **3c** and **3e**, respectively. None of the most active THIQs in D_2 DR displayed relevant cytotoxicity in human neutrophils and HUVEC. Finally, and in agreement with the experimental data, molecular modeling studies on DRs of the most characteristic ligands of the three series revealed stronger molecular interactions with D_2 DR than with D_1 DR, which further supports to the encountered enhanced selectivity to D_2 DR.

1. Introduction

The tetrahydroisoquinoline (THIQ) structure has been identified in a wide range of isoquinoline (IQ) alkaloids distributed in several botanical families and marine animals [1,2]. This family of alkaloids has been linked to important pharmacological activities, including antitumor, antibiotic [3], β-adrenergic [4], α-glucosidase inhibition [5], NMDA [6] and dopamine receptors ligands [7–19].

Dopamine is a neurotransmitter that plays a key role in several psychiatric and neurological disorders, and affects numerous people worldwide. Modulation of the dopaminergic activity that acts at dopamine receptors (DR) as potential targets for treating schizophrenia or Parkinson's disease is an area of enormous interest. Therefore, the discovery of new dopaminergic ligands as potential drug candidates for the treatment of these psychiatric and neurological disorders is widely required [20,21]. DRs can be classified into two pharmacological families (D_1 and D_2-like) that include five DR (D_1-like: D_1 and D_5; D_2-like: D_2, D_3 and D_4). Therapeutically, the D_2-like DR antagonists have been seen to be effective to treat schizophrenia (antipsychotics) and agonists in the treatment of Parkinson's disease symptoms [20,21]. Although the

* Corresponding author. Institute of Health Research-INCLIVA, University Clinic Hospital of Valencia, 46010, Valencia, Spain
** Corresponding author. Departamento de Farmacología, Laboratorio de Farmacoquímica, Facultad de Farmacia, Universidad de Valencia, 46100, Burjassot, Valencia, Spain.
E-mail addresses: ncabedo@uv.es (N. Cabedo), dcortes@uv.es (D. Cortes).

http://dx.doi.org/10.1016/j.ejmech.2016.06.009
0223-5234/

pathophysiology of depression has been allocated to serotonin and noradrenaline systems, nowadays the dopaminergic system also seems to play an important role in this disorder [22,23]. Besides dopamine re-uptake inhibitors, different selective D_2-like DR agonists have been found to display antidepressant-like behavioral effects in several rodent models [24].

For several decades our research group has reported that THIQs, which are closely related to the dopamine structure, have an affinity for DR [7–19]. In these studies, we determined the relevance of different substituents in the IQ ring on DR affinity [11–16]. Presence of hydroxyl groups in the A-ring increases affinity to both D_1-like and D_2-like DR families, whereas their blockade decreases it. Affinity and selectivity to DR have been found to be modulated by the presence of a secondary or tertiary amine in the THIQ structure [9–16]. Molecular modeling studies have revealed the importance of hydrophobic motifs since they seem to enhance their DR affinity [17,18]. Recently, we introduced a new methodology to generate the unusual 1,2,3,7,8,8a-hexahydrocyclopenta[*ij*]isoquinoline (HCPIQ) skeleton [19] by Friedel-Crafts cyclization with Eaton's reagent [25]. Tricyclic HCPIQ appears as an original scaffold that contains a THIQ core connected to a cyclopentane motif and a phenyl substituent. Preliminary results have indicated that this semi-rigid structure has extraordinary affinity to DR [19], which encourages us to carry out structure-activity relationship (SAR) and molecular modeling studies. To this end, we prepared three series: (*E*)-1-styryl-1,2,3,4-THIQs (series 1), 7-phenyl-1,2,3,7,8,8a-hexahydrocyclopenta[*ij*]-IQs (series 2) and (*E*)-1-(prop-1-en-1-yl)-1,2,3,4-THIQs (series 3) (Fig. 1) and we evaluated their potential dopaminergic activity. The present study was designed to shed light onto the significant groups that can affect the dopaminergic activity of the HCPIQ skeleton. Based on previous SAR studies with dopaminergic IQ [16,26,27], we evaluated the effect of different substituents on the nitrogen atom (*N*H, *N*-methyl and *N*-allyl) and dioxygenated-IQ functions (*O*-methyl and catechol), the substituent at the β-position of the THIQ skeleton (methyl or phenyl) and the effect of the presence or absence of the cyclopentane ring on both D_1-like and D_2-like DR affinity. The toxicity of the most promising compounds was also evaluated. The MTT ((3-(4,5-dimethylthiazol-2-yl)-2,5-diphenyltetrazolium bromide) assay and the cytofluorometric analysis were performed to determine their impact on human cell apoptosis and survival. Finally, in order to assess the different molecular interactions that can stabilize or destabilize the distinct ligand-receptor complexes in both receptor types, molecular modeling studies that simulated the molecular interactions of the most characteristic ligands of each series with both D_2 and D_1 DR were carried out.

2. Results and discussion

2.1. Chemistry

The synthesis of THIQs (series 1 and 3) and HCPIQs (series 2) was carried out as shown in the Schemes 1 and 2. THIQs (series 1) and HCPIQs (series 2) (Scheme 1) were synthesized from 2-(3,4-dimethoxyphenyl)ethylamine as starting material under Schotten-Baumann conditions to generate *N*-(3,4-dimethoxyphenethyl)cinnamamide (**1**) [28,29]. Next, cinnamamide (**1**) was converted into the corresponding THIQ (**2**) by the Bischler-Napieralski cyclodehydration reaction using $POCl_3$ in dry acetonitrile, followed by $NaBH_4$ reduction [9]. Once obtained, the (*E*)-6,7-dimethoxy-1-styryl-1,2,3,4-THIQ (**2**) was subjected to Friedel–Crafts cyclization conditions using Eaton's Reagent [25] (P_2O_5–CH_3SO_3H, 1:10, w/w) to generate the corresponding 5,6-dimethoxy-7-phenyl-HCPIQ (**3**) (Scheme 1).

(*E*)-1-(Propenyl)-1,2,3,4-THIQs (series 3, Scheme 2) was synthesized by a similar approach to that described above. The starting material was also 2-(3,4-dimethoxyphenyl)ethylamine, but was subjected to Schotten-Baumann conditions with crotonoyl chloride to generate (*E*)-*N*-(3,4-dimethoxyphenethyl)but-2-enamide (**4**) [15]. Amide **4** was treated with $POCl_3$ followed by reduction with $NaBH_4$, to obtain (*E*)-6,7-dimethoxy-1-(prop-1-en-1-yl)-1,2,3,4-THIQ (**5**) [9]. It seemed that the absence of the electron donating group, such as the benzene ring in the series 3, prevented Friedel-Crafts cyclization from take place. Therefore, the cyclopentane ring did not form under these conditions.

After synthesizing THIQs **2** (series 1), **3** (series 2) and **5** (series 3), methyl or allyl substituents were introduced into the nitrogen atom to obtain tertiary amines. We obtained, on the one hand, the corresponding *N*-methyl THIQs **2b**, **3b** and **5b** using formaldehyde and formic acid, and subsequent $NaBH_4$ reduction and, on the other hand, the corresponding *N*-allyl-THIQs **2d**, **3d** and **5d** using allyl chloride under basic conditions with K_2CO_3.

Finally, all the THIQs (**2**, **2b**, **2d**, **3**, **3b**, **3d**, **5**, **5b** and **5d**) were *O*-demethylated by the addition of four equivalents of BBr_3 reagent for 2 h at room temperature [14] to obtain (*E*)-1-styryl-1,2,3,4-THIQs-6,7-diol (**2a**, **2c**, **2e** for series 1) and 7-phenyl-HCPIQs-5,6-diol (**3a**, **3c**, **3e** for series 2) and (*E*)-1-(propenyl)-1,2,3,4-THIQs-6,7-diol (**5a**, **5c**, **5e** for series 3) with good yields.

2.2. Binding affinities for dopamine receptors: structure-activity relationship

The synthesized THIQs were assayed *in vitro* for their ability to displace the selective radioligands of D_1 and D_2 DR from their respective specific binding sites in striatal membranes. Dopamine was used as the reference compound. All the synthetized

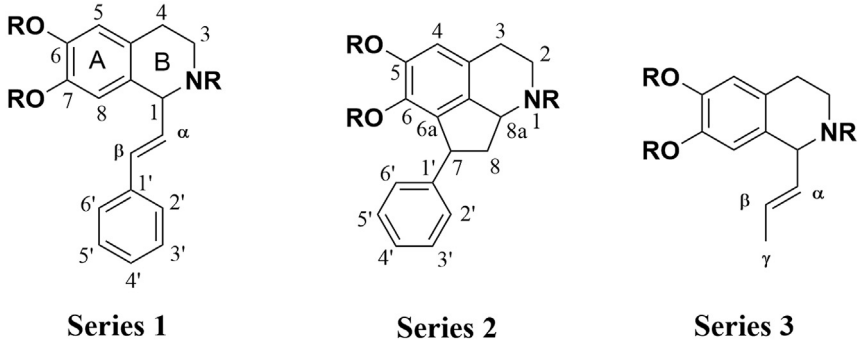

Fig. 1. 1-Styryl-THIQ (series 1), HCPIQ (series 2) and 1-propenyl-THIQ (series 3).

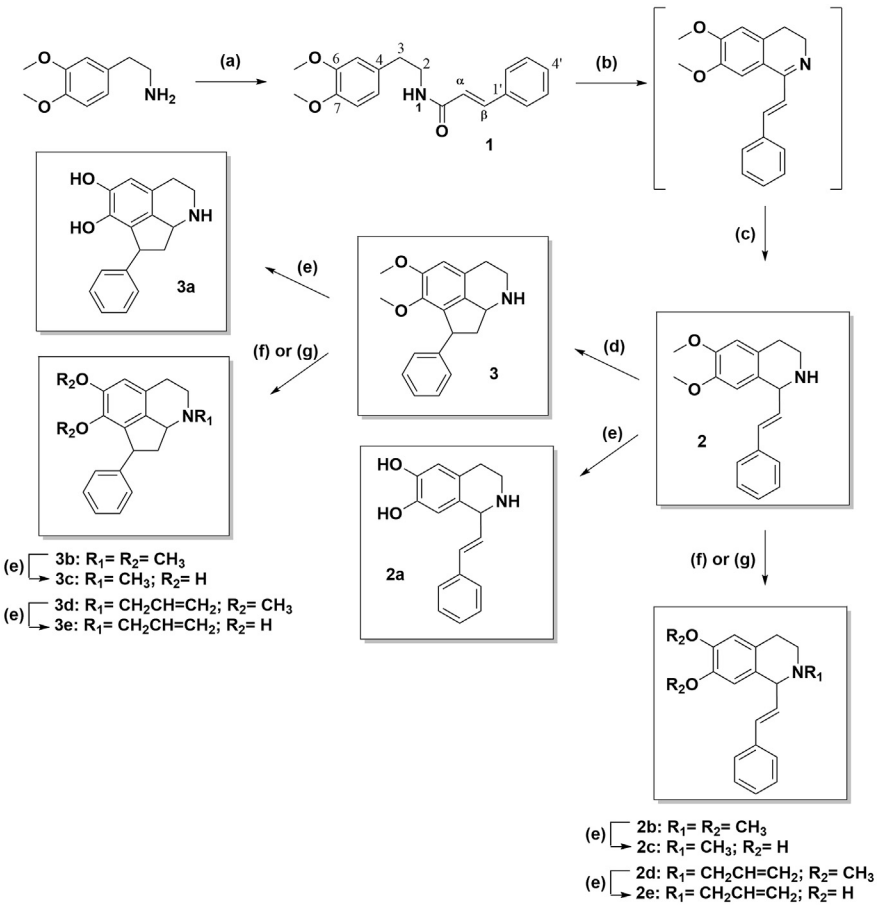

Scheme 1. Synthesis of 1-styryl-THIQs **2** and **2a**-**e** (series 1), and HCPIQs **3** and **3a**-**e** (series 2). Reagents and Conditions: (a) cinnamoyl chloride, CH_2Cl_2, 5% NaOH, rt, 3h; (b) $POCl_3$, CH_3CN, N_2, reflux, 5h; (c) $NaBH_4$; MeOH, rt, 2h; (d) Eaton's Reagent, reflux, 15h; (e) CH_2Cl_2, BBr_3, rt, 2h; (f) CH_3OH, CH_2O, HCO_2H, reflux, 1h; followed by $NaBH_4$, reflux, 1h; (g) allyl chloride, K_2CO_3, CH_3CN, reflux, 10h.

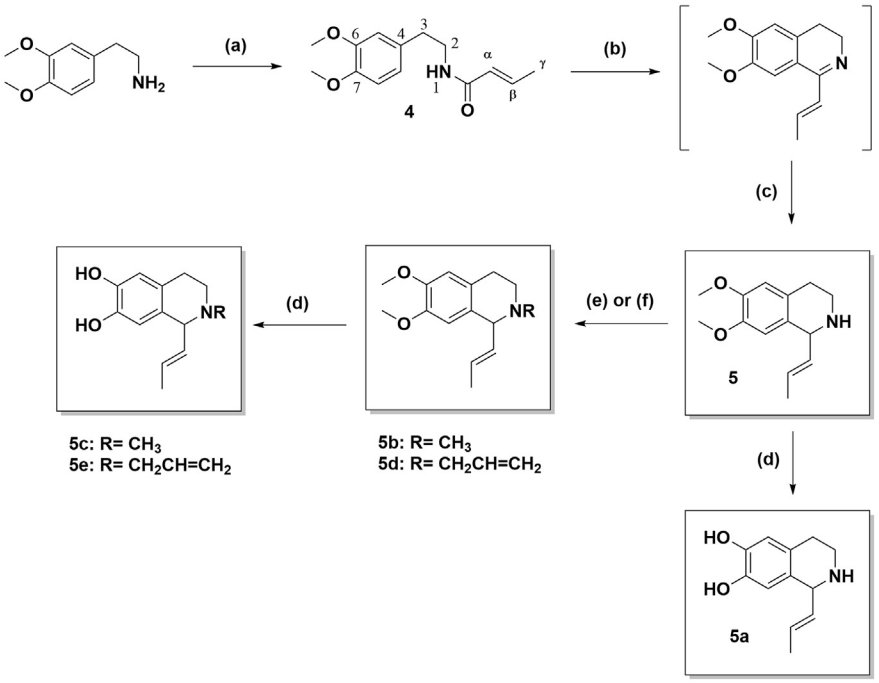

Scheme 2. Synthesis of (*E*)-1-(propenyl)-1,2,3,4-THIQs **5** and **5a**-**e** (series 3). Reagents and Conditions: (a) crotonoyl chloride, CH_2Cl_2, 5% NaOH, rt, 3h; (b) $POCl_3$, CH_3CN, N_2, reflux, 5h; (c) $NaBH_4$; MeOH, rt, 2h; (d) CH_2Cl_2, BBr_3, rt, 2h; (e) CH_3OH, CH_2O, HCO_2H, reflux, 1h; followed by $NaBH_4$, reflux, 1h; (f) allyl chloride, K_2CO_3, CH_3CN, reflux, 10 h.

compounds were able to displace [^{3}H]-SCH 23390 (a selective D_1-like DR radioligand) from its specific binding sites at micromolar concentrations (μM). Although dopamine showed a Ki value of 0.55 μM for D_1 DR, the compounds of series 1 (**2**,**2a**-**e**) displayed Ki values between 3.18 and 9.57 μM, and two compounds of series 3, **5c** and **5e** had Ki = 1.28 and 1.71 μM, respectively. Indeed both series 1 and 3 possessed a more flexible structure than series 2 to accommodate the binding pocket of D_1 DR. However, several compounds from series 1, 2 and 3 were able to displace [^{3}H]-raclopride (a selective D_2-like DR radioligand) from its specific binding sites at nanomolar (nM) concentrations, with 10–30 fold more affinity for D_2 DR than for dopamine (see Table 1 for the binding affinities for D_1 and D_2 DR).

2.2.1. Effect of dioxygenated substituents in the THIQ and HCPIQ nucleus

In general, all the tested *O*-methylated THIQs, including the HCPIQs, showed a lower affinity to D_1 and D_2 DR than their corresponding homologs with a free catecholic group (see Table 1 and Fig. 2), probably because of the possibility of forming hydrogen bond interactions between catecholic hydroxyls and amino acid residues (Ser193 and Ser197) at the D_2 DR binding pocket (described below in the molecular modeling studies).

2.2.2. Effect of the N-substitution

N-substitution was performed by introducing a methyl or allyl group. The obtained results suggested that substitution for a methyl or allyl group did not affect affinity to DR since no significant differences were obtained. Therefore, it seemed that the affinity and the selectivity for DR of the secondary or tertiary amines relied on the presence or absence of catecholic groups in each THIQ structure. Despite these findings, a different affinity to D_1 or D_2 DR was found in each synthesized series: a) in series 1, N-substitution increased the affinity for D_2 DR in both compounds 6,7-dimethoxy (**2** *vs*. **2d**) and 6,7-dihydroxy (**2a** *vs*. **2e**, Fig. 3); b) in series 2, N-substitution in compounds 5,6-dihydroxy almost did not change the D_2 DR affinity (**3a** *vs*. **3e**, Fig. 3) and preserved the high affinity within the nanomolar range; c) in series 3, N-substitution in compounds 6,7-dihydroxy increased the affinity to both DRs (**5a** *vs*. **5e**, Fig. 3). Perhaps the reason was because, besides the salt bridge between the protonated nitrogen atom of THIQ and Asp103, and Asp114 for D_1 and D_2 DR, respectively, there were additional hydrophobic interactions between compounds/DRs (in general, more with the D_2) which contributed to the stabilization process (described below in molecular modeling studies). This apparently affected series 1 and 3 slightly more.

2.2.3. Effect of the substituent at the β-position of 1-substituted THIQ (series 1 and 3)

The comparison made between series 1 and 3 with a different substituent at the β-position of THIQs (methyl or phenyl) allowed us to demonstrate that the nature of the substituent affected ligand DR binding. In fact, the aromatic substituents at this position increased the affinity for both D_1 and D_2 DR. This effect was observed in both compounds *O*-methylated and 6,7-dihydroxy (Fig. 4). It could be related to the highest electronic density and the steric hindrance of the aromatic group *vs*. methyl, which could favor hydrophobic interactions with certain amino acids (depending on D_1 or D_2 DR) that promote stabilization to compound/DR complexes (mentioned below in the molecular modeling studies).

2.2.4. Effect of presence or absence of a cyclopentane on THIQ

Presence of a cyclopentane ring revealed a marked increase in selectivity to D_2 DR, with D_1/D_2 ratio values of 2465, 1010 and 382 for **3a**, **3c** and **3e** (Fig. 5), respectively, which sharply contrasted with the most active and selective compounds of series 1 and 3, with Ki D_1/D_2 ratios of 56 for **2c**, 147 for **2e**, 18 for **5c** and 95 for **5e** (Table 1). The best selectivity of series 2 was explained by the rigidity of this skeleton.

Table 1
Values of affinity (K_i, pK_i) and ratio Ki D_1/D_2 determined in binding experiments to D_1 and D_2 DR of series 1, 2 and 3.

THIQ	Specific ligand D_1 [^{3}H]-SCH 23390		Specific ligand D_2 [^{3}H]-raclopride		Ki D_1/D_2
	Ki (μM)	pKi	Ki (μM)	pKi	
Dopamine	0.550 ± 0.023	6.260 ± 0.059	0.560 ± 0.009	6.837 ± 0.028	0.98
2	4.556 ± 0.862	5.360 ± 0.094	6.176 ± 1.717	5.244 ± 0.123	0.74
2a	9.571 ± 0.227	5.048 ± 0.119	1.422 ± 0.316	5.869 ± 0.099^{d}	6.73^{b}
2b	6.200 ± 1.907	5.251 ± 0.137	0.436 ± 0.081	6.376 ± 0.088^{d}	14.22^{b}
2c	3.185 ± 0.159	5.498 ± 0.022	**0.057 ± 0.013**	**7.264 ± 0.094**^{e,g}	**55.87**^{c}
2d	7.679 ± 1.670	5.133 ± 0.087	1.166 ± 0.172	5.942 ± 0.066^{d,h}	6.58^{b}
2e	6.038 ± 2.025	5.267 ± 0.144	**0.041 ± 0.010**	**7.408 ± 0.097**^{e,m}	**147.3**^{c}
3	33.373 ± 6.891	4.499 ± 0.104^{d}	10.977 ± 1.933	4.972 ± 0.071	3.04^{a}
3a	71.493 ± 16.281	4.174 ± 0.117^{e}	**0.029 ± 0.009**	**7.593 ± 0.184**^{e,q}	**2465.3**^{c}
3b	23.780 ± 4.549	4.640 ± 0.084^{h}	4.188 ± 1.348	5.422 ± 0.137^{g,r}	5.67^{b}
3c	13.136 ± 2.452	4.895 ± 0.076^{k,s}	**0.013 ± 0.002**	**7.890 ± 0.083**^{i,t}	**1010.5**^{c}
3d	18.620 ± 4.822	4.758 ± 0.109	3.514 ± 0.654	5.472 ± 0.092^{n,r}	5.29^{b}
3e	6.873 ± 1.391	5.179 ± 0.085^{s}	**0.018 ± 0.007**	**7.800 ± 0.160**^{p,u}	**381.8**^{c}
5	45.610 ± 5.548	4.347 ± 0.050^{d}	8.855 ± 1.154	5.059 ± 0.054	5.15^{b}
5a	57.670 ± 7.457	4.246 ± 0.057^{e}	0.458 ± 0.081	6.352 ± 0.077^{f,v}	125.9^{c}
5b	18.286 ± 1.501	4.740 ± 0.034^{i,w}	14.696 ± 0.609	4.833 ± 0.018^{g}	1.24
5c	1.286 ± 0.153	5.897 ± 0.054^{l,x,y}	**0.072 ± 0.023**	**7.181 ± 0.129**^{x,y}	**17.86**^{c}
5d	37.650 ± 4.798	4.432 ± 0.059^{m}	13.816 ± 0.634	4.860 ± 0.019^{m}	2.72^{a}
5e	1.714 ± 0.095	5.766 ± 0.025$^{o,x,a'}$	**0.018 ± 0.002**	**7.749 ± 0.069**$^{p,x,z,a'}$	**95.2**^{c}

Data were displayed as mean ± SEM for 3 experiments.
Values of **3**-**3e** from previous publication [19].
ANOVA, post Newmann-Keuls multiple comparison tests:
$^{a}p < 0.05$ vs D_1-like dopaminergic receptor. $^{b}p < 0.01$ vs D_1-like dopaminergic receptor. $^{c}p < 0.001$ vs D_1-like dopaminergic receptor. $^{d}p < 0.001$ vs **2**. $^{e}p < 0.001$ vs **2a**. $^{f}p < 0.01$ vs **2a**. $^{g}p < 0.001$ vs **2b**. $^{h}p < 0.01$ vs **2b**. $^{i}p < 0.05$ vs **2b**. $^{j}p < 0.001$ vs **2c**. $^{k}p < 0.01$ vs **2c**. $^{l}p < 0.05$ vs **2c**. $^{m}p < 0.001$ vs **2d**. $^{n}p < 0.05$ vs **2d**. $^{o}p < 0.01$ vs **2e**. $^{p}p < 0.05$ vs **2e**. $^{q}p < 0.001$ vs **3**. $^{r}p < 0.05$ vs **3**. $^{s}p < 0.001$ vs **3a**. $^{t}p < 0.001$ vs **3b**. $^{u}p < 0.001$ vs **3d**. $^{v}p < 0.001$ vs **5**. $^{w}p < 0.01$ vs **5**. $^{x}p < 0.001$ vs **5a**. $^{y}p < 0.001$ vs **5b**. $^{z}p < 0.001$ vs **5c**. $^{a'}p < 0.001$ vs **5d**.
Bold is to remark the good results

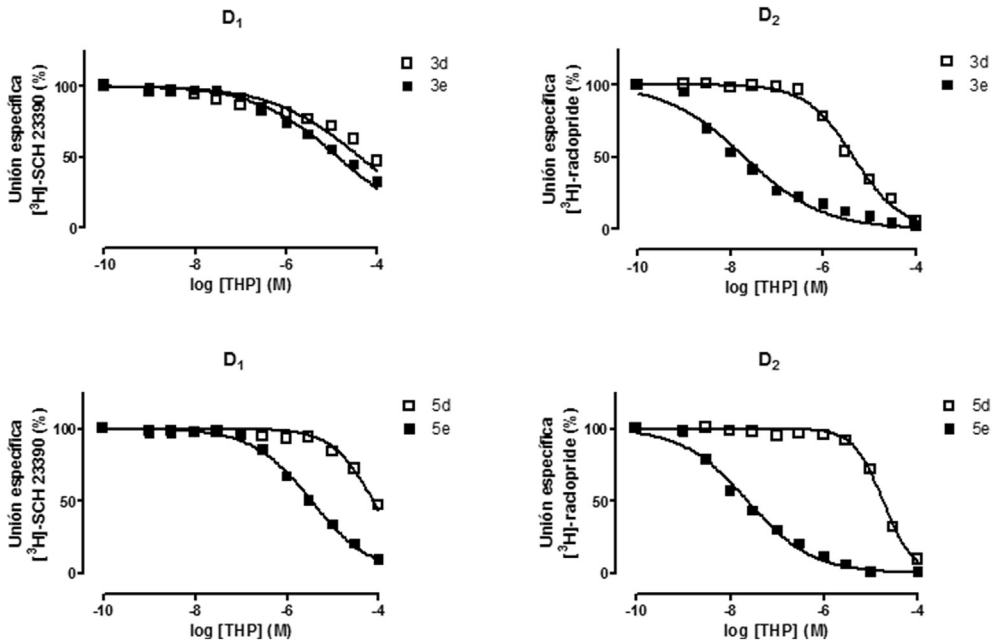

Fig. 2. Displacement curves of [^{3}H]-SCH 23390 (D_1) and [^{3}H] raclopride (D_2) specific binding by compounds **3d** vs **3e** and **5d** vs **5e**. Data are presented as mean ± SEM of n = 3 independent experiments.

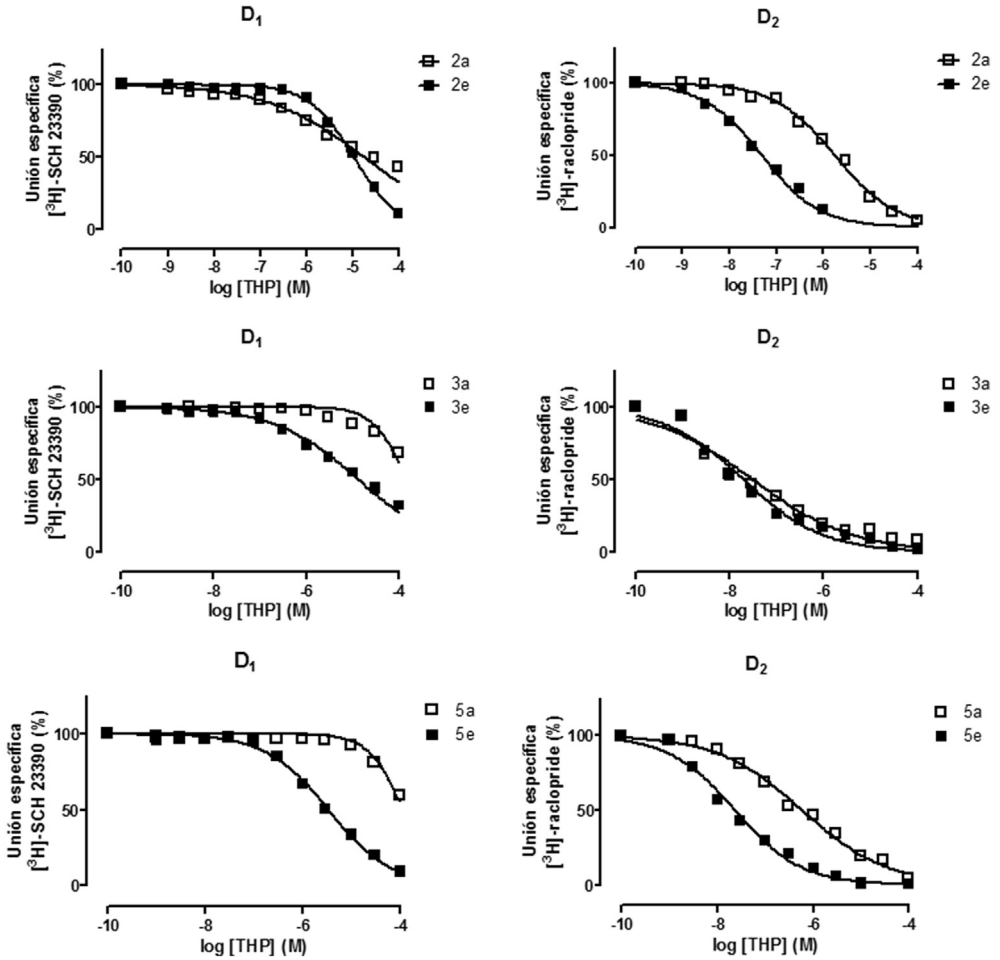

Fig. 3. Displacement curves of [^{3}H]-SCH 23390 (D_1) and [^{3}H] raclopride (D_2) specific binding by compounds **2a** vs **2e** (series 1), **3a** vs **3e** (series 2) and **5a** vs **5e** (series 3). Data are presented as mean ± SEM of n = 3 independent experiments.

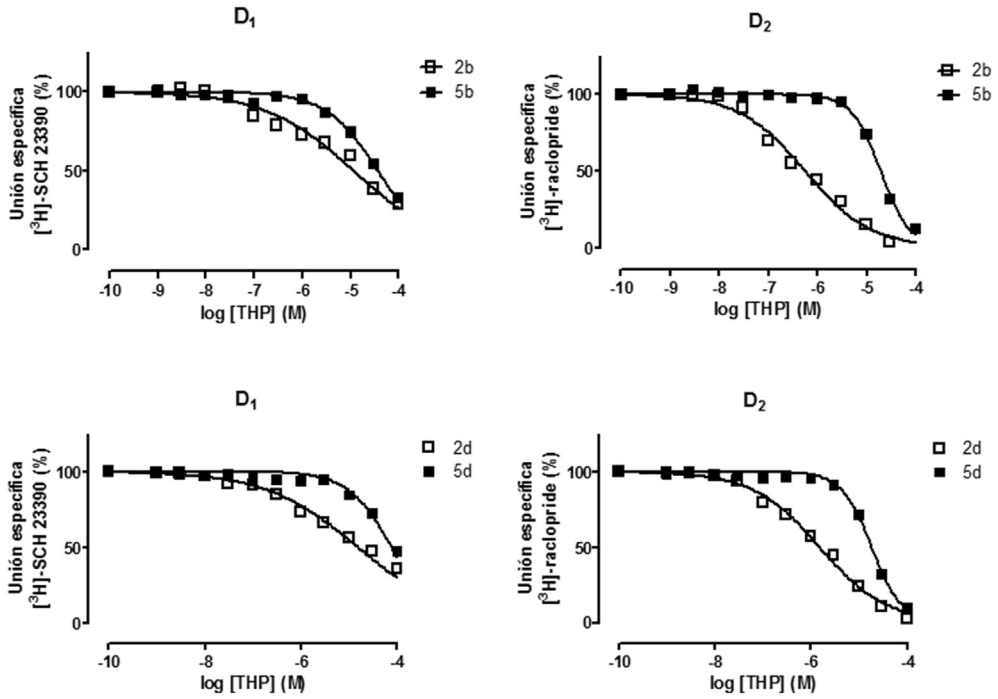

Fig. 4. Displacement curves of [^{3}H]-SCH 23390 (D_1) and [^{3}H] raclopride (D_2) specific binding by compounds **2b** vs **5b** and **2d** vs **5d**. Data are presented as mean ± SEM of n = 3 independent experiments.

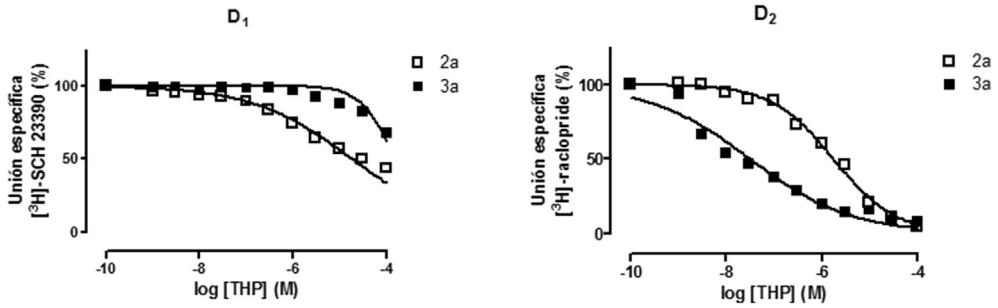

Fig. 5. Displacement curves of [^{3}H]-SCH 23390 (D_1) and [^{3}H] raclopride (D_2) specific binding by compounds **2a** vs **3a**. Data are presented as mean ± SEM of n = 3 independent experiments.

2.3. Cytotoxicity assays

After determining the affinity to the DRs of the synthesized THIQs, the cytotoxicity of the most active compounds in D_2 DR (**2c**, **2e**, **3a**, **3c**, **3e**, **5c** and **5e**) was determined at 30 μM by the MTT assay run on human neutrophils and primary cell cultures of human umbilical vein endothelial cells (HUVEC). The MTT assay done with HUVEC showed that the tested compounds did not displayed any cytotoxicity, while in neutrophils only **3e** had a significant effect (Fig. 6). It is noteworthy that **3a**, the most D_2 selective compound, did not display cytotoxicity in either neutrophils or HUVEC at 30 μM.

To confirm the cytotoxic effect of these THIQs, we investigated the effect on neutrophil and HUVEC apoptosis, and the survival of these most D_2 DR active compounds (**2c**, **2e**, **3a**, **3c**, **3e**, **5c** and **5e**). For this purpose, a cytofluorimetric method was employed. It should be noted that most of the tested THIQs did not exhibit cytotoxicity at the assayed concentration (30 μM) in either neutrophils or HUVEC (Fig. 7).

2.4. Molecular modeling

To better understand selectivity to D_2-like DR, we performed a molecular modeling study with the most characteristic ligands of each series and compounds **2c**, **2e**, **3c**, **3e**, **5c** and **5e** (see Schemes 1 and 2) were selected. We herein simulated the molecular interactions of these ligands with both receptors D_1 and D_2 to assess the different molecular interactions that can stabilize or destabilize the distinct ligand-receptor complexes. The molecular modeling study was conducted in four different stages. In the first step, a docking analysis was performed by the Autodock program [30]. The compounds of series 1 and 3 only had one chiral center, whereas those of series 2 presented two chiral carbons. Therefore, the different enantiomers of each series were taken into account. Our simulations also considered the possibility of the up or down position of the substituents in the *N* of amine group. In a second stage, molecular dynamics (MD) simulations were performed using the AMBER software package. Once again, all the different enantiomers of each series were considered in these simulations. Our results indicated that *S* enantiomer was the energetically preferred form

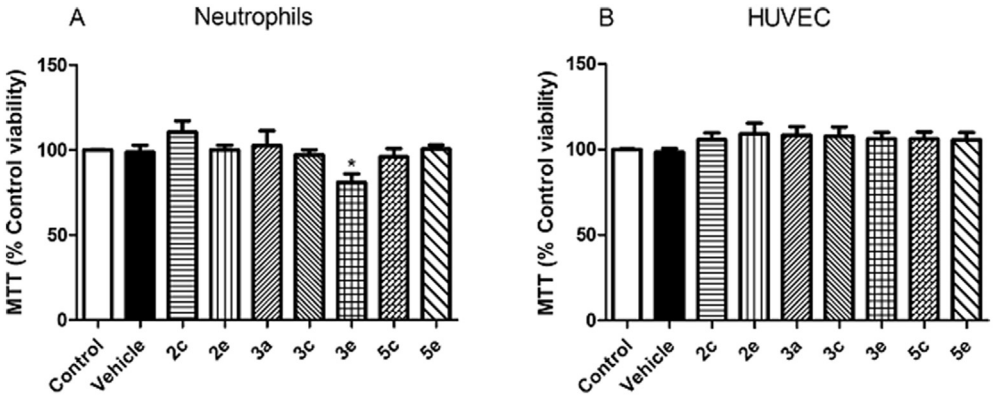

Fig. 6. Effect of the synthesized THIQs on human neutrophil (A) and HUVEC (B) viability. Data are presented as mean ± SEM of n = 3 independent experiments. *p < 0.05 relative to the vehicle group.

for series 1 and 3, while *R*, *S* was the preferred form for series 2. It is important to note that these theoretical results agree with those previously reported for the compounds structurally related to series 1 and 3 [14,15,18], and with those for series 2 [19]. Based on the data obtained with the MD simulations, the most representative structures of each complex were selected by the cluster tool implemented in the AMBER package [31]. Each structure was optimized by employing hybrid method ONIOM [32]. Finally, a QTAIM [33] study was carried out for the QM layers of the different optimized complexes.

In general, the compounds herein studied displayed their pharmacophoric portions in a closely related spatial form to that reported for dopamine [17,34] and other dopaminergic ligands [35]. Consistently with previous experimental [36] and theoretical [37] data, the simulations indicated the relevance of negatively charged aspartate 114 and 103 for D_2 and D_1 DR ligand binding, respectively. In line with this, ligand binding to highly conserved aspartic acid indicated that the terminal carboxyl group could function as an anchoring point for the molecules that possess a protonated amino group [36–39]. In fact, all the simulated compounds were docked into the receptor with the protonated amino group close to Asp114 for D_2 DR, and to Asp103 for D_1 DR. After 1.5 ns of MD simulations, ligands slightly and differently moved from the initial position, but the strong interactions with both aspartate residues were maintained for all the complexes. These results further supported the role of aspartate residues as anchoring points for ligands with a protonated amino group.

Since the different interactions that stabilize and destabilize the formation of complexes with both receptors (D_1 and D_2) are relatively weak, and MD simulations are not accurate enough to distinguish the different affinities observed experimentally, additional studies were carried out. To do so, hybrid calculations (QM/MM) and a subsequent QTAIM study were performed. Fig. 8 provides the values obtained for ρ for the six selected compounds, which formed complexes with the two receptor types. Clearly all the compounds that established complexes with D_2 DR had higher ρ values than those observed with D_1 DR. These theoretical results fully coincided with the experimental data and could explain, at least in part, the higher affinities displayed by these three series of compounds for D_2 DR. To better understand this differential behavior at the molecular level, an analysis of the ρ value for each residue was performed to discriminate their contribution to complex interactions. Figs. 9–11 show the values of ρ obtained for the different molecular interactions of the complexes of compounds **2e**, **3e** and **5e** with both receptors D_1 and D_2. These figures illustrate clear molecular interactions between these compounds and Asp114 and Ser193 at D_2 DR, which are significantly stronger than those established with Asp103 and Ser198 at D_1 DR. Once these compounds were complexed with D_2 DR, additional hydrophobic interactions (Val115, Ile183, Ile184, Trp386, Phe389, Phe390, His393, Thr412 and Tyr416) were detected, which favored stabilization to the compound/receptor complexes. Although similar hydrophobic interactions (Ile104, Asn185, Leu190, Phe288 and Trp321) were established with D_1 DR, they were much weaker than those for D_2 DR. Similar results were detected for the complexes established with compounds **2c, 3c** and **5c** (these results are shown in Figs. 1S–3S as Supplementary Material).

Next the molecular graphs obtained for the different compound/receptor complexes were analyze by QTAIM techniques and the intermolecular interactions were evaluated. Here the results obtained for compound **2e** are discussed since similar approaches can be applied for the remainding compounds (see Figs. 4S–7S, Supporting Information). Fig. 12 shows the main stabilizing interactions such as Asp114 and Ser193 for D_2 DR and Asp103 and Ser198 for D_1 DR, whereas Fig. 13 illustrates the most relevant hydrophobic interactions that contribute to the stabilization process. Since the active site at D_1 DR was greater than at D_2 DR [40,41], it is likely that compound interactions were favored to D_2 DR *vs.* D_1 (Fig. 12). Regarding the complexes shown in Fig. 13, more hydrophobic interactions were found with D_2 DR than with D_1 DR (nine *vs.* five residues, respectively). Furthermore, the compound/D_2 DR interactions at the active site were stronger than those at D_1 DR. Similar data were obtained for compounds **3e** and **5e** (Figs. 5S and 7S, Supplementary Material). Taken together, the molecular modeling study clearly indicated that the three series of compounds herein evaluated established stronger molecular interactions with D_2 DR than with D_1 which is consistent with the presented experimental data and partly explained the selectivity detected to the former DR.

3. Conclusions

In summary, we synthesized three series of IQs: (*E*)-1-styryl-1,2,3,4-THIQs (series 1), 7-phenyl-1,2,3,7,8,8a-HCPIQs (series 2) and (*E*)-1-(prop-1-en-1-yl)-1,2,3,4-THIQs (series 3) with different substituents on the nitrogen atom (methyl or allyl), the dioxygenated function (methoxyl or catechol groups), the substituent at the β-position of the THIQ skeleton and presence of the cyclopentane motif. We evaluated the SAR for their potential dopaminergic affinity (D_1 and D_2-like DR). Presence of hydroxyls groups into the IQ-ring resulted in increased affinity to DRs, while their blockade was detrimental. Regarding N-substitution, the tertiary amines

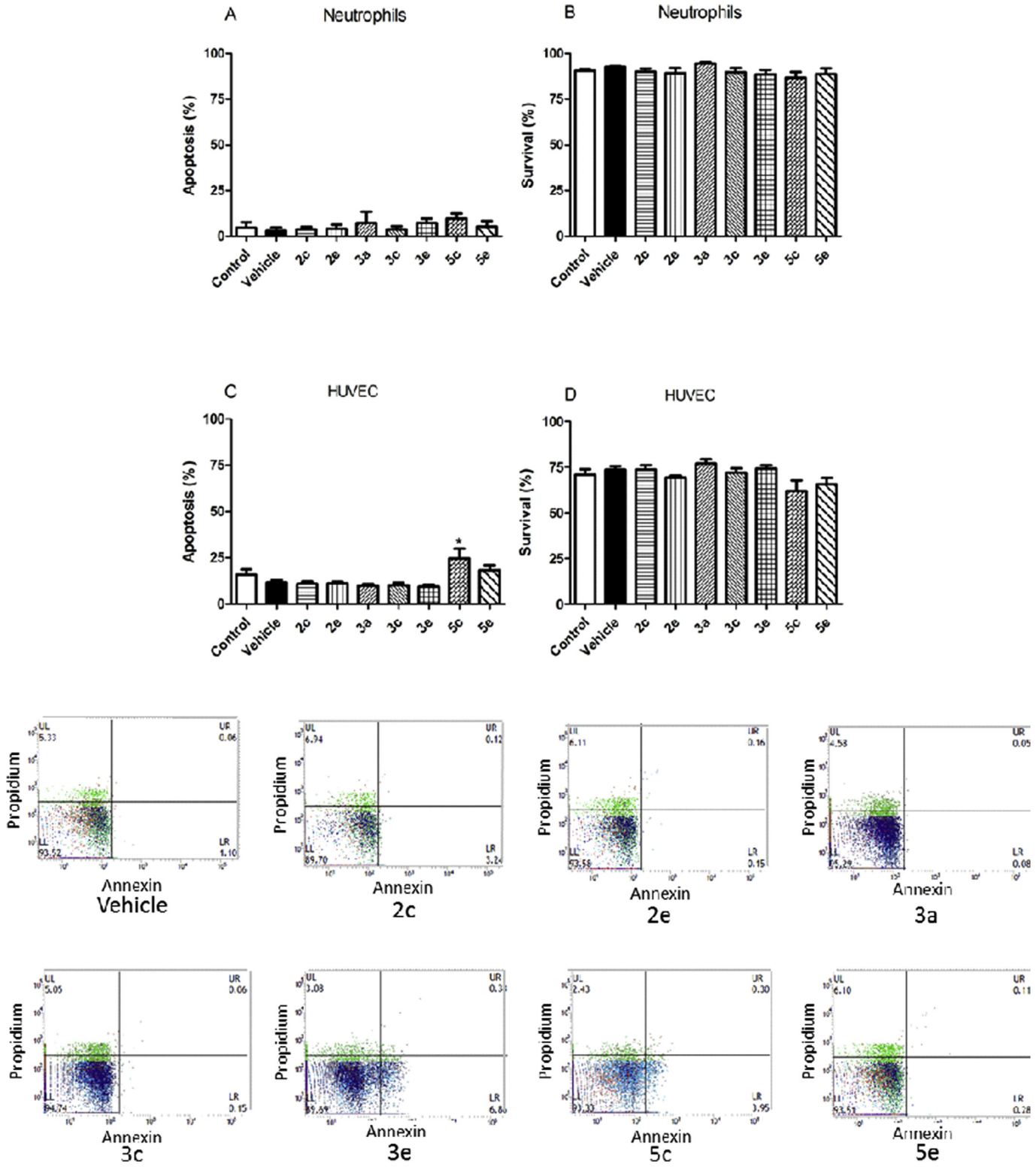

Fig. 7. Percentage of apoptotic (**A**) and survival neutrophils (**B**) and apoptotic (**C**) and survival HUVEC (**D**) after 24 h incubation with THIQs. Apoptotic cells were quantified as the percentage of total population of annexin V+, PI− cells, late apoptotic, and/or necrotic cells as annexin V+ and PI+, and viable nonapoptotic cells as annexin V− and PI−. Representative flow cytometry panels showing the effects of vehicle, **2c**, **2e**, **3a**, **3c**, **3e**, **5c** and **5e** on neutrophil apoptosis/survival have been included. The columns are the mean ± SEM of n = 3 independent experiments. *$p < 0.05$ relative to the vehicle group.

improved affinity to DR compared to their corresponding secondary amines. Finally, of our series, the phenyl group at the β position of 1-substituted THIQs in series 1 increased the affinity to DRs compared with the 1-alkyl-THIQs (series 3). It was noteworthy that the presence of the cyclopentane motif (tricyclic HCPIQs, series 2) generated the most active compounds, which displayed

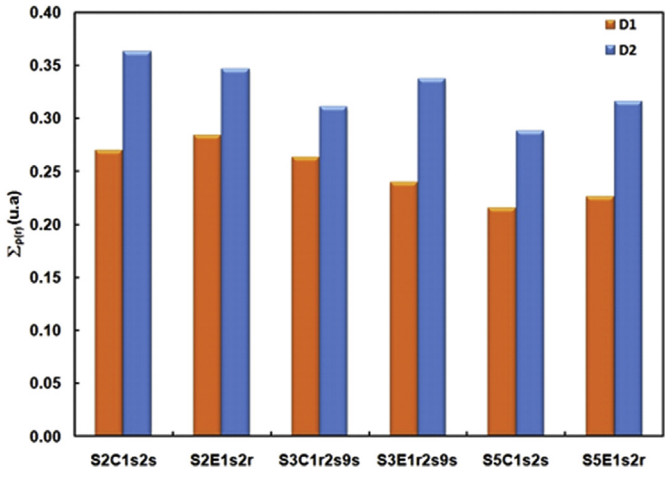

Fig. 8. Sum of the values of charge density ($\sum\rho_{(r)}$) at the bond critical points obtained for the different compounds. The interactions are shown in orange for D_1 DR and in blue for D_2 DR. (For interpretation of the references to colour in this figure legend, the reader is referred to the web version of this article.)

astonishing selectivity to D_2-DR. None of the most active THIQs in D_2 DR (**2c**, **2e**, **3a**, **3c**, **3e**, **5c**, and **5e**) displayed any relevant cytotoxicity on both human neutrophils and HUVEC. Finally, the molecular modeling study results were consistent with the experimental data and provided further details about the molecular interactions that stabilized the compound/DR complexes.

4. Experimental section

4.1. General instrumentation

EIMS and FAB mass were recorded on a VG Auto Spec Fisons spectrometer instruments (Fisons, Manchester, United Kingdom). ^{1}H NMR and ^{13}C NMR spectra were recorded with $CDCl_3$ or Methanol-d_4 as a solvent on a Bruker AC-300, AC-400 or AC-500. Multiplicities of ^{13}C NMR resonances were assigned by DEPT experiments. COSY, HSQC and HMBC correlations were recorded at 400 MHz and 500 MHz (Bruker AC-400° AC-500). The assignments of all compounds were made by COSY, DEPT, HSQC and HMBC. All the reactions were monitored by analytical TLC by silica gel 60 F_{254} (Merck 5554). Residues were purified by silica gel 60 (40–63 μm, Merck 9385) column chromatography. Quoted yields are of purified material. The HCl salts of the synthesized compounds were prepared from the corresponding base with 5% HCl in MeOH.

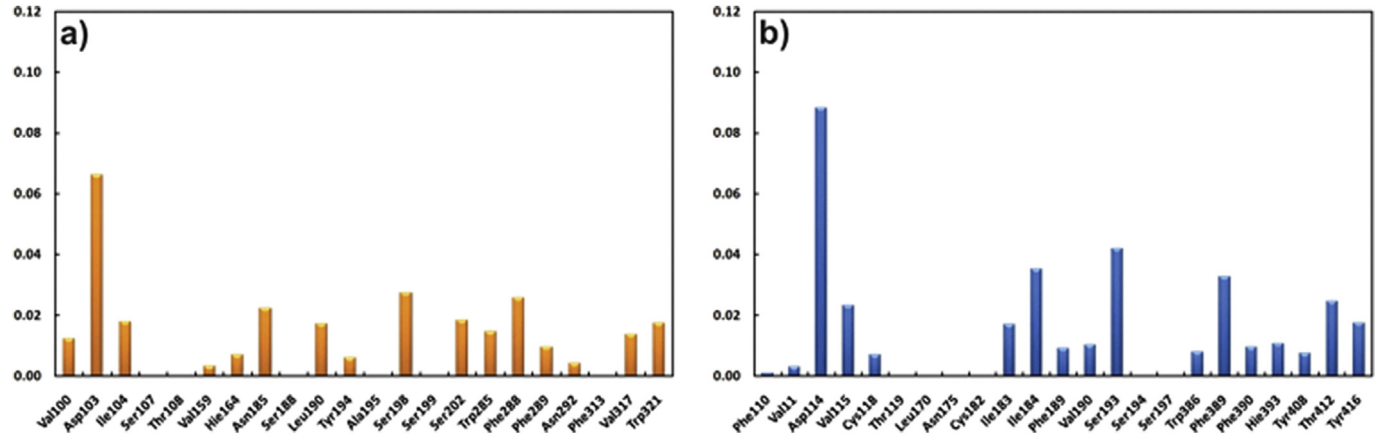

Fig. 9. Sum of the values of charge density ($\sum\rho(r)$) at the bond critical points between compound **2e** and the different residues of D_1 DR (a) and D_2 DR (b). Only the inter-molecular interactions have been considered.

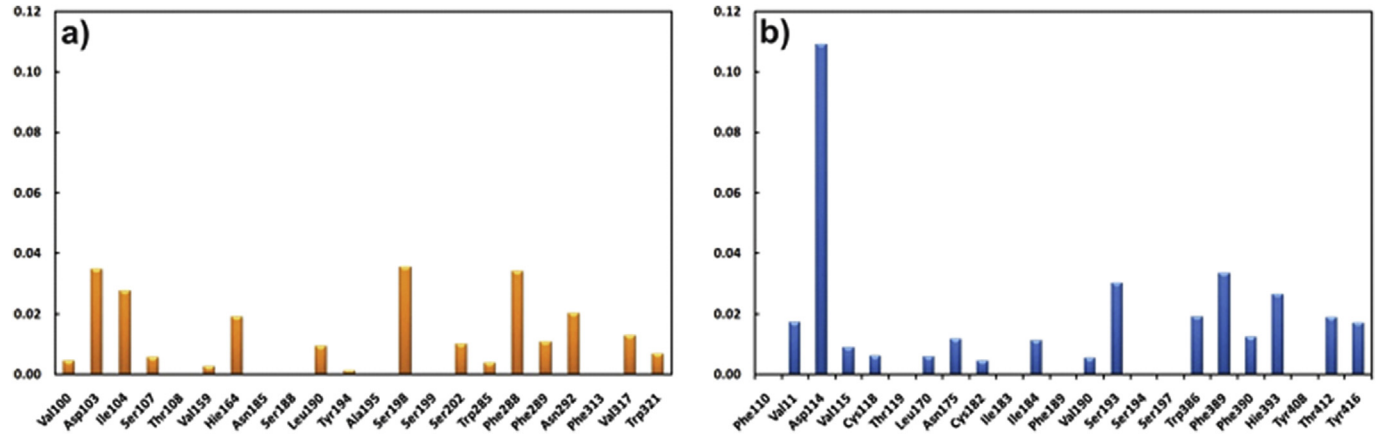

Fig. 10. Sum of the values of charge density ($\sum\rho(r)$) at the bond critical points between compound **3e** and the residues of D_1 DR (a) and D_2 DR (b).

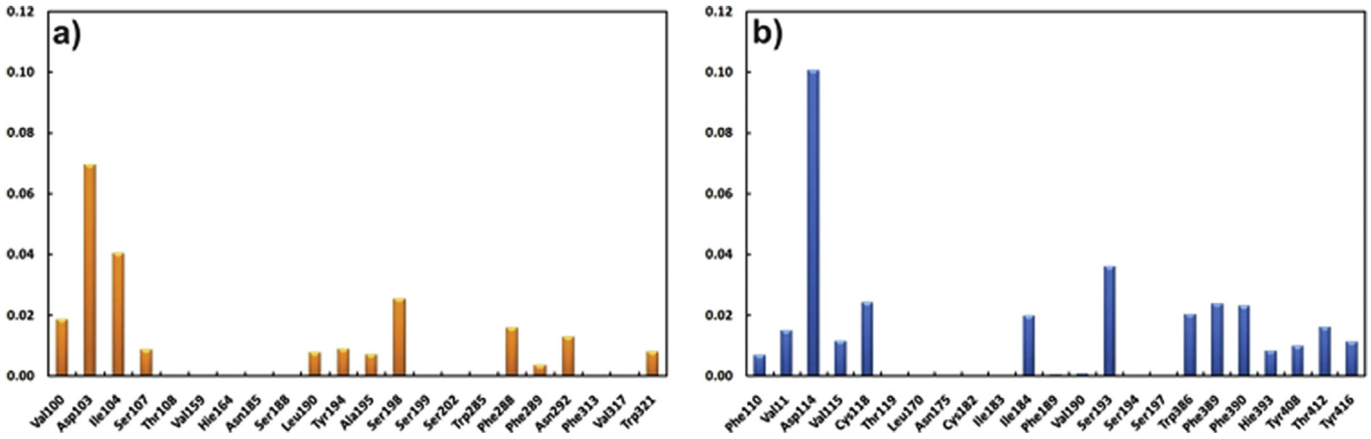

Fig. 11. Sum of the values of charge density ($\sum\rho(r)$) at the bond critical points between compound **5e** and the residues of D_1 DR (a) and D_2 DR (b).

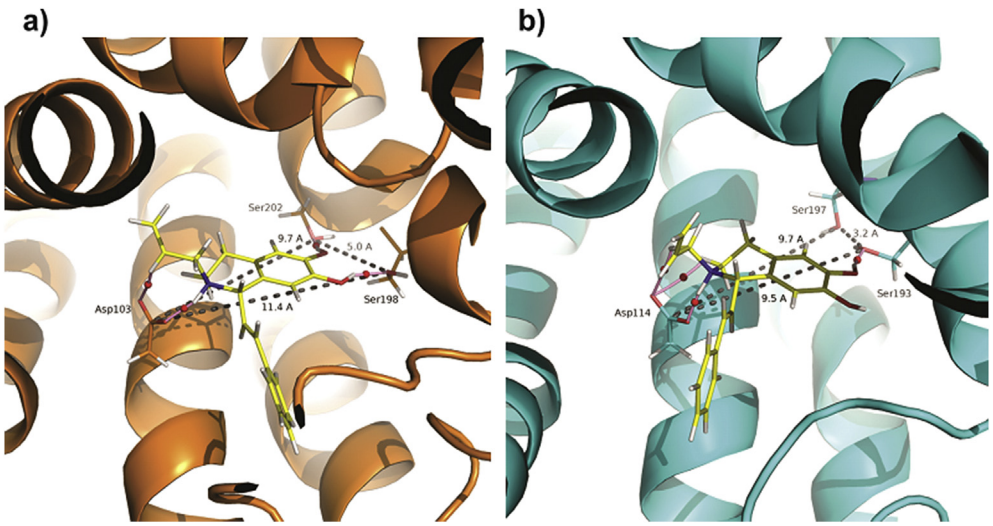

Fig. 12. Molecular graph of the non-covalent interactions between compound **2e** and main residues. a) Asp103, Ser198 and Ser202 of D_1 DR. b) Asp114, Ser193 and Ser197 of D_2 DR. The elements of the topology of the electron density are shown: pink spheres represent the bond paths connecting the nuclei and the critical bond points are represented as red spheres. The triangle in dot lines shows the interatomic distances obtained for the main residues. (For interpretation of the references to colour in this figure legend, the reader is referred to the web version of this article.)

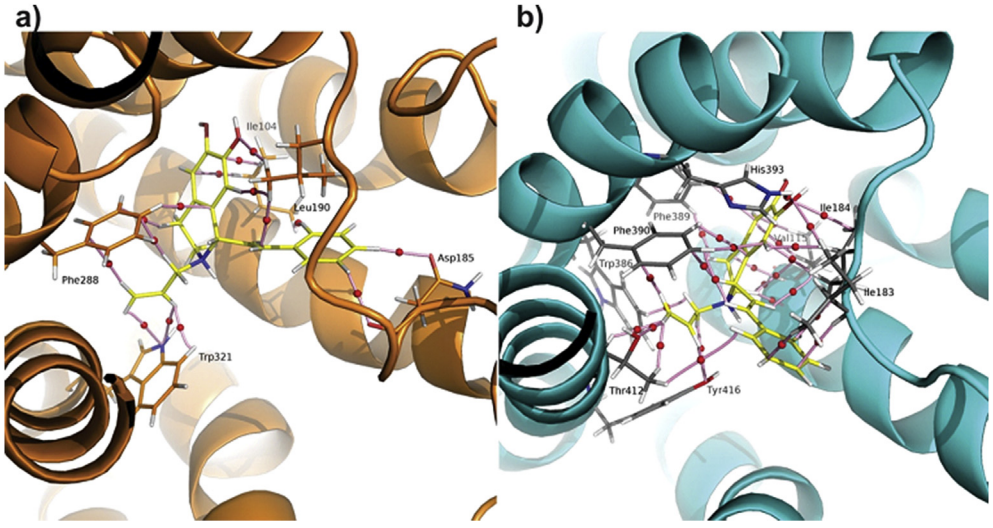

Fig. 13. Molecular graph of the molecular interactions between compound **2e** and hydrophobic residues. a)Ile104, Asn185, Leu190, Phe288 and Trp321 of D_1 DR. b) Val115, Ile183, Ile184, Trp386, Phe389, Phe390, His393, Thr412 and Tyr416 of D_2 DR.

4.2. Chemistry

4.2.1. General procedure for the synthesis of acetamides (**1** and **4**) under Schotten-Baumann conditions

Formation of acetamides was carried out under Schotten-Baumann conditions using 2-(3,4-dimethoxyphenyl)ethanamine and the corresponding acid chloride.

*4.2.1.1. N-(3,4-dimethoxyphenethyl)cinnamamide (**1**).* An amount of 458 mg of cinnamoyl chloride (2.76 mmol) dissolved in CH_2Cl_2 (1 mL) was added dropwise at 0 °C to a solution of 2-(3,4-dimethoxyphenyl)ethylamine (500 mg, 2.76 mmol) in CH_2Cl_2 (20 mL) and 5% aqueous NaOH (4.4 mL) with stirring at room temperature for 3 h. Then, the mixture was stirred with 2.5% aqueous HCl. The organic solution was washed with brine (2 × 10 ml) and H_2O (2 × 10 ml), dried over anhydrous Na_2SO_4 and evaporated to dryness. The residue obtained was purified by silica gel column chromatography (Hexane/CH_2Cl_2/EtOAc, 20:70:10) to afford the acetamide **1** (781 mg, 91%) as a white oil. ^{1}H NMR (500 MHz, $CDCl_3$): δ = 7.62 (d, J = 15.6 Hz, 1H, CH-β), 7.44 (m, 2H, CH-2′ and CH-6′), 7.31 (m, 3H, CH-3′, CH-4′ and CH-5′), 6.79 (d, J = 7.9 Hz, 1H, CH-8), 6.74 (d, J = 7.9 Hz, 1H, CH-9), 6.73 (s, 1H, CH-5), 6.37 (d, J = 15.6 Hz, 1H, CH-α), 6.02 (m, 1H, NH), 3.84 (s, 3H, OCH_3-6), 3.83 (s, 3H, OCH_3-7), 3.62 (q, J = 7.0 Hz, 2H, CH_2-2), 2.83 (t, J = 7.0 Hz, 2H, CH_2-3); ^{13}C NMR (125 MHz, $CDCl_3$): δ = 165.9 (CO), 148.9 (C-6), 147.6 (C-7), 140.8 (CH-β), 134.7 (C-1′), 131.3 (C-4), 129.5 (CH-4′), 128.9 (CH-3′ and CH-5′), 127.6 (CH-2′ and CH-6′), 120.7 (CH-9), 120.6 (CH-α), 111.9 (CH-5), 111.3 (CH-8), 55.8 (OCH_3-6), 55.7 (OCH_3-7), 40.9 (CH_2-2), 35.1 (CH_2-3); MS (FAB) m/z (%): 312 $[M+H]^+$, 295 (20), 165 (20), 131 (100).

*4.2.1.2. (E)-N-(3,4-dimethoxyphenethyl)but-2-enamide (**4**).* 2-(3,4-Dimethoxyphenyl)-ethylamine (500 mg, 2.76 mmol) and crotonoyl chloride (0.26 mL, 2.76 mmol) were subjected to similar conditions to those described above to obtain the compound **1**. The residue was purified by silica gel column chromatography (Hexane/CH_2Cl_2/EtOAc, 20:70:10) to obtain the acetamide **4** (642 mg, 93%) as a white oil. ^{1}H NMR (500 MHz, $CDCl_3$): δ = 6.82 (m, 1H, CH-β), 6.77 (m, 1H, CH-9), 6.71 (m, 1H, CH-8), 6.68 (m, 1H, CH-5), 5.70 (d, J = 15.1, 1H, CH-α), 5.52 (m, 1H, NH), 3.84 (s, 3H, OCH_3-6), 3.83 (s, 3H, OCH_3-7), 3.51 (q, J = 7.0 Hz, 2H, CH_2-2), 2.75 (t, J = 7.0 Hz, 2H, CH_2-3), 1.80 (dd, J = 6.1, 1.7 Hz, 3H, CH_3-γ); ^{13}C NMR (125 MHz, $CDCl_3$): δ = 165.9 (CO), 148.9 (C-6), 147.6 (C-7), 139.7 (CH-β), 131.4 (C-4), 125.0 (CH-α), 120.6 (CH-9), 111.9 (CH-5), 111.3 (CH-8), 55.8 (OCH_3-6), 55.7 (OCH_3-7), 40.6 (CH_2-2), 35.4 (CH_2-3), 17.6 (CH_3-γ); MS (FAB) m/z (%): 272 $[M+Na]^+$, 254 (50), 135 (20).

4.2.2. General procedure for the synthesis of 1,2,3,4-tetrahydroisoquinoleines (**2** and **5**) by Bischler-Napieralski cyclization

*4.2.2.1. (E)-6,7-Dimethoxy-1-styryl-1,2,3,4-tetrahydroisoquinoline (**2**).* The corresponding acetamide **1** (500 mg, 1.61 mmol) was added in dry acetonitrile (40 mL) to a 100 mL three-neck round-bottom flask at 0 °C under N_2, and treated with $POCl_3$ (1.15 mL, 11.2 mmol). The mixture was stirred and refluxed under N_2 for 5 h and then cooled to room temperature. Acetonitrile was evaporated under reduced pressure and the reaction mixture was slowly poured into a mixture of crushed ice. The solid residue was neutralized with 10% aqueous NaOH to obtain a suspension (pH ≈ 8–9) which was then extracted with CH_2Cl_2 (3 × 15 mL). Combined CH_2Cl_2 layers were dried over Na_2SO_4 and the solvent was evaporated *in vacuo* obtaining reddish oil. The residue was dissolved in MeOH (10 mL), and then it was treated with $NaBH_4$ (189 mg, 5 mmol). The reaction mixture was stirred for 2 h. Next, water (15 mL) was added and methanol evaporated under reduced pressure. The aqueous phase was extracted with CH_2Cl_2 (3 × 15 ml), and combined organic layers were dried over Na_2SO_4 and evaporated to dryness. The crude product was purified by silica gel column chromatography (CH_2Cl_2/MeOH, 95:5) to furnish the compound **2** (383 mg, 81%) as a yellow oil. ^{1}H NMR (500 MHz, $CDCl_3$): δ = 7.40 (d, J = 7.6 Hz, 2H, CH-2′ and CH-6′), 7.29 (t, J = 7.6 Hz, 2H, CH-3′ and CH-5′), 7.24 (t, J = 7.6 Hz, 1H, CH-4′), 6.62 (s, 1H, CH-8), 6.60 (s, 1H, CH-5), 6.58 (d, J = 14.8 Hz, 1H, CH-β), 6.35 (dd, J = 14.8, 8.0 Hz, 1H, CH-α), 4.60 (d, J = 8.0 Hz, 1H, CH-1), 3.84 (s, 3H, OCH_3-7), 3.78 (s, 3H, OCH_3-6), 3.28 (m, 1H, CH-3α), 3.07 (m, 1H, CH-3β), 2.85 (m, 1H, CH-4α), 2.62 (m, 1H, CH-4β); ^{13}C NMR (125 MHz, $CDCl_3$): δ = 147.7 (C-7), 147.1 (C-6), 136.8 (C-1′), 132.3 (CH-β), 131.9 (CH-α), 128.5 (C-8a), 128.4 (CH-2′ and CH-6′), 127.6 (CH-3′ and CH-5′), 126.9 (C-4a), 126.5 (CH-4′), 111.7 (CH-8), 110.4 (CH-5), 59.1 (CH-1), 55.9 (OCH_3-6), 55.8 (OCH_3-7), 41.5 (CH_2-3), 29.0 (CH_2-4); MS (FAB) m/z (%): 296 $[M+H]^+$, 279 (100), 200 (20), 151 (30); HRESIMS m/z 296.1644 $[M+H]^+$ (296.1651, calc for $C_{19}H_{22}NO_2$).

*4.2.2.2. (E)-6,7-Dimethoxy-1-(prop-1-en-1-yl)-1,2,3,4-tetrahydroisoquinoline (**5**).*

(*E*)-*N*-(3,4-dimethoxyphenethyl)but-2-enamide (500 mg, 2.00 mmol) was subjected to similar conditions to those described above to obtain the THIQ **2**. The residue was purified by silica gel column chromatography (CH_2Cl_2/MeOH, 95:5) to afford the compound **5** (410 mg, 88%) as a yellow oil. ^{1}H NMR (500 MHz, $CDCl_3$): δ = 6.56 (s, 1H, CH-5), 6.54 (s, 1H, CH-8), 5.73 (dd, J = 15.2, 7.7 Hz, 1H, CH-β), 5.62 (dd, J = 15.2, 7.9 Hz, 1H, CH-α), 4.45 (d, J = 7.9 Hz, 1H, CH-1), 3.83 (s, 3H, OCH_3-7), 3.80 (s, 3H, OCH_3-6), 3.25 (m, 1H, CH-3α), 3.06 (m, 1H, CH-3β), 2.84 (m, 1H, CH-4α), 2.72 (m, 1H, CH-4β), 1.74 (dd, J = 7.7, 1.4 Hz, 3H, CH_3-γ); ^{13}C NMR (125 MHz, $CDCl_3$): δ = 147.8 (C-7), 147.2 (C-6), 132.2 (CH-α), 129.7 (CH-β), 128.1 (C-8a), 126.3 (C-4a), 111.5 (CH-8), 110.5 (CH-5), 58.6 (CH-1), 55.9 (OCH_3-6), 55.8 (OCH_3-7), 41.0 (CH_2-3), 28.3 (CH_2-4), 17.7 (CH_3-γ); MS (FAB) m/z (%): 234 $[M+H]^+$, 217 (100), 189 (20); HRESIMS m/z 234.1486 $[M+H]^+$ (234.1494, calc for $C_{14}H_{20}NO_2$).

4.2.3. General procedure for Friedel–Crafts cyclization

*4.2.3.1. 5,6-Dimethoxy-7-phenyl-1,2,3,7,8,8a-hexahydrocyclopenta[ij]isoquinoline (**3**).* 5 mL of Eaton's Reagent was used to dissolve an amount of 500 mg of (*E*)-6,7-dimethoxy-1-styryl-1,2,3,4-tetrahydroisoquinoline (**2**) (1.69 mmol) at room temperature and the reaction mixture was stirred at 45 °C overnight. Then, 5% aqueous NaOH was added and the mixture was then extracted with CH_2Cl_2 (3 × 15 mL). Combined CH_2Cl_2 layers were dried over Na_2SO_4 and the solvent was evaporated *in vacuo* obtaining reddish oil. The residue obtained was purified by silica gel column chromatography (CH_2Cl_2/MeOH, 95:5) to afford the hexahydrocyclopenta-IQ **3** (339 mg, 68%) as a brown oil. ^{1}H NMR and HRESIMS [19]; ^{13}C NMR (125 MHz, $CDCl_3$): δ = 152.7 (C-6a), 143.9 (C-6), 143.8 (C-5), 135.6 (C-1′), 134.7 (C-3a^1), 128.3 (CH-3′ and CH-5′), 127.3 (CH-2′ and CH-6′), 126.8 (C-3a), 126.0 (CH-4′), 111.0 (CH-4), 60.3 (OCH_3-5), 57.5 (CH-8a), 56.1 (OCH_3-6), 46.3 (CH-7), 44.6 (CH_2-2), 44.4 (CH_2-8), 25.8 (CH_2-3); MS (FAB) m/z (%): 296 $[M+H]^+$, 279 (100), 267 (20), 192 (30), 151 (30).

4.2.4. General procedure for N-methylation

*4.2.4.1. (E)-6,7-Dimethoxy-2-methyl-1-styryl-1,2,3,4-tetrahydroisoquinoline (**2b**).* To a stirred solution of **2** (100 mg, 0.34 mmol) in MeOH (15 mL), 37% formaldehyde (4.7 mL) and one drop of formic acid were added. The mixture was refluxed for 1 h, cooled to room temperature, treated with $NaBH_4$ (120 mg, 3.4 mmol), and refluxed an additional hour. The reaction mixture was cooled to room temperature and the solvent was removed under reduced pressure. Then, water (3 mL) was added, and the

aqueous mixture was extracted with CH_2Cl_2 (3 × 15 mL). Combined organic layers were dried over Na_2SO_4 and concentrated under reduced pressure to give the crude residue which was further purified by silica gel column chromatography (CH_2Cl_2/MeOH, 98:2) to afford the compound **2b** (83 mg, 79%). ^{1}H NMR (500 MHz, $CDCl_3$): δ = 7.42 (d, J = 7.5 Hz, 2H, CH-2′ and CH-6′), 7.31 (t, J = 7.5 Hz, 2H, CH-3′ and CH-5′), 7.25 (m, 1H, CH-4′), 6.62 (s, 1H, CH-8), 6.61 (s, 1H, CH-5), 6.59 (d, J = 15.8 Hz, 1H, CH-β), 6.14 (dd, J = 15.8, 8.9 Hz, 1H, CH-α), 3.85 (s, 3H, OCH_3-7), 3.81 (m, 1H, CH-1), 3.74 (s, 3H, OCH_3-6), 3.09 (m, 1H, CH-3α), 3.05 (m, 1H, CH-4α), 2.74 (m, 1H, CH-4β), 2.57 (m, 1H, CH-3β), 2.46 (s, 3H, NCH_3); ^{13}C NMR (125 MHz, $CDCl_3$): δ = 147.5 (C-7), 147.0 (C-6), 136.6 (C-1′), 133.1 (CH-β), 131.3 (CH-α), 128.3 (CH-3′ and CH-5′), 128.1 (C-8a), 127.4 (CH-4′), 126.4 (C-4a), 126.3 (CH-2′ and CH-6′), 111.1 (CH-8), 110.7 (CH-5), 68.4 (CH-1), 55.7 (OCH_3-6), 55.0 (OCH_3-7), 51.2 (CH_2-3), 44.0 (NCH_3), 28.7 (CH_2-4); MS (FAB) m/z (%): 310 $[M+H]^+$, 279 (90), 206 (50), 201 (50), 151 (100); HRESIMS m/z 310.1793 $[M+H]^+$ (310.1807, calc for $C_{20}H_{24}NO_2$).

*4.2.4.2. 5,6-dimethoxy-1-methyl-7-phenyl-1,2,3,7,8,8a-hexahydrocyclopenta-[ij]isoquinoline (**3b**).*

5,6-Dimethoxy-7-phenyl-1,2,3,7,8,8a-hexahydrocyclopenta-[*ij*]-isoquinoline (**3**) (100 mg, 0.34 mmol) was subjected to similar conditions to those described above to obtain the compound **2b**. The residue was purified by silica gel column chromatography (CH_2Cl_2/MeOH, 95:5) to afford the THIQ **3b** (86 mg, 82%) as a white oil [19]. ^{1}H NMR (500 MHz, $CDCl_3$): δ = 7.18 (m, 2H, CH-3′ and CH-5′), 7.09 (m, 2H, CH-2′ and CH-6′), 7.08 (m, 1H, CH-4′), 6.53 (s, 1H, CH-4), 4.51 (d, J = 8.4 Hz, 1H, CH-7), 3.74 (s, 3H, OCH_3-5), 3.48 (s, 3H, OCH_3-6), 3.33 (dd, J = 9.8, 6.6 Hz, 1H, CH-8a), 3.05 (dd, J = 12.0, 6.6 Hz, 1H, CH-2α), 2.89 (m, 1H, CH-3α), 2.72 (m, 1H, CH-3β), 2.42 (m, 1H, CH-2β), 2.31 (m, 1H, CH_2-8), 2.26 (s, 1H, NCH_3); ^{13}C NMR (125 MHz, $CDCl_3$): δ = 152.7 (C-6a), 144.1 (C-6), 144.0 (C-5), 135.1 (C-1′), 128.4 (CH-3′ and CH-5′), 128.1 (C-3a^1), 127.5 (CH-2′ and CH-6′), 127.4 (C-3a), 126.1 (CH-4′), 110.6 (CH-4), 65.7 (CH-8a), 60.3 (OCH_3-6), 56.1 (OCH_3-5), 54.8 (CH_2-2), 46.4 (CH-7), 43.6 (CH_2-8), 43.2 (NCH_3), 27.2 (CH_2-3); MS (FAB) m/z (%): 310 $[M+H]^+$, 291 (45), 267 (100), 206 (45); HRESIMS m/z 310.1797 $[M+H]^+$ (310.1807, calc for $C_{20}H_{24}NO_2$).

*4.2.4.3. (E)-6,7-Dimethoxy-2-methyl-1-(prop-1-en-1-yl)-1,2,3,4-tetrahydroisoquinoline (**5b**).*

(*E*)-6,7-Dimethoxy-1-(prop-1-en-1-yl)-1,2,3,4-tetrahydroisoquinoline (**5**) (100 mg, 0.43 mmol) was subjected to similar conditions to those described above to obtain the THIQ **2b** and **3b**. The residue was purified by silica gel column chromatography (CH_2Cl_2/MeOH, 95:5) to afford the compound **5b** (91 mg, 86%) as a white oil. ^{1}H NMR (500 MHz, $CDCl_3$): δ = 6.56 (s, 1H, CH-5), 6.55 (s, 1H, CH-8), 5.68 (dt, J = 15.1, 6.4 Hz, 1H, CH-β), 5.35 (dd, J = 15.1, 8.8 Hz, 1H, CH-α), 3.82 (s, 3H, OCH_3-7), 3.79 (s, 3H, OCH_3-6), 3.59 (d, J = 8.8 Hz, 1H, CH-1), 2.98 (m, 1H, CH-3α), 2.91 (m, 1H, CH-4α), 2.66 (m, 1H, CH-4β), 2.48 (m, 1H, CH-3β), 2.38 (s, 3H, NCH_3), 1.76 (dd, J = 6.4, 1.6 Hz, 3H, CH_3-γ); ^{13}C NMR 7(125 MHz, $CDCl_3$): δ = 147.5 (C-7), 146.9 (C-6), 132.7 (CH-α), 129.2 (CH-β), 128.8 (C-8a), 126.3 (C-4a), 111.1 (CH-8), 110.8 (CH-5), 68.3 (CH-1), 55.8 (OCH_3-6), 55.7 (OCH_3-7), 51.2 (CH_2-3), 43.9 (NCH_3), 28.7 (CH_2-4), 17.6 (CH_3-γ); MS (FAB) m/z (%): 270 $[M+Na]^+$, 213 (10); HRESIMS m/z 248.1647 $[M+H]^+$ (248.1651, calc for $C_{15}H_{22}NO_2$).

4.2.5. General procedure for N-allylation

*4.2.5.1. (E)-2-Allyl-6,7-dimethoxy-1-styryl-1,2,3,4-tetrahydroisoquinoline (**2d**).* To a stirred solution of **2** (100 mg, 0.34 mmol) in CH_3CN (10 mL), K_2CO_3 (300 mg, 2.17 mmol) and allyl chloride (0.1 mL, 1.23 mmol) were added. The mixture was refluxed for 10 h. The reaction mixture was cooled to room temperature and the solvent removed under reduced pressure. Then, water (3 mL) was added and the aqueous mixture was extracted with CH_2Cl_2 (3 × 15 mL). Combined organic layers were dried over Na_2SO_4 and concentrated under reduced pressure to give the crude residue which was further purified by silica gel column chromatography (CH_2Cl_2/MeOH 99:1) to afford the THIQ **2d** (97 mg, 87%) as a white oil. ^{1}H NMR (500 MHz, $CDCl_3$): δ = 7.33 (d, J = 7.2 Hz, 2H, CH-2′ and CH-6′), 7.23 (t, J = 7.2 Hz, 2H, CH-3′ and CH-5′), 7.15 (m, 1H, CH-4′), 6.54 (s, 1H, CH-8), 6.52 (s, 1H, CH-5), 6.48 (d, J = 15.8 Hz, 1H, CH-β), 6.14 (dd, J = 15.8, 8.6 Hz, 1H, CH-α), 5.86 (m, 1H, CH-2″), 5.14 (d, J = 17.2 Hz, 1H, CH-3″α), 5.10 (d, J = 10.2 Hz, 1H, CH-3″β), 4.09 (d, J = 8.6 Hz, 1H, CH-1), 3.81 (s, 3H, OCH_3-7), 3.67 (s, 3H, OCH_3-6), 3.41 (dd, J = 13.9, 5.4 Hz, 1H, CH-1″α), 3.05 (m, 1H, CH-3α), 3.00 (dd, J = 13.9, 7.5 Hz, 1H, CH-1″β), 2.80 (m, 1H, CH-4α), 2.72 (m, 1H, CH-4β), 2.54 (m, 1H, CH-3β); ^{13}C NMR (125 MHz, $CDCl_3$): δ = 147.7 (C-7), 147.1 (C-6), 136.8 (C-1′), 135.6 (CH-2″), 133.1 (CH-β), 131.1 (CH-α), 128.5 (CH-2′ and CH-6′), 128.3 (C-8a), 127.5 (CH-4′), 126.7 (C-4a), 126.4 (CH-3′ and CH-5′), 117.7 (CH_2-3″), 111.3 (CH-8), 111.1 (CH-5), 65.4 (CH-1), 57.7 (CH_2-1″), 55.9 (OCH_3-6), 55.8 (OCH_3-7), 46.3 (CH_2-3), 28.4 (CH_2-4); MS (FAB) m/z (%): 336 $[M+H]^+$, 281 (20), 189 (15), 151 (100); HRESIMS m/z 336.1953 $[M+H]^+$ (336.1964, calc for $C_{22}H_{26}NO_2$).

*4.2.5.2. 1-Allyl-5,6-dimethoxy-7-phenyl-1,2,3,7,8,8a-hexahydrocyclopenta[ij]-isoquinoline (**3d**).*

5,6-Dimethoxy-7-phenyl-1,2,3,7,8,8a-hexahydrocyclopenta-[*ij*]-isoquinoline (**3**) (100 mg, 0.34 mmol) was subjected to similar conditions to those described above to obtain the THIQ **2d**. The residue was purified by silica gel column chromatography (CH_2Cl_2/MeOH, 99:1) to afford compound **3d** (101 mg, 89%) as a brown oil [19]. ^{1}H NMR (500 MHz, $CDCl_3$): δ = 7.18 (m, 2H, CH-3′ and CH-5′), 7.10 (m, 2H, CH-2′ and CH-6′), 7.08 (m, 1H, CH-4′), 6.53 (s, 1H, CH-4), 5.82 (m, 1H, CH-2″), 5.11 (d, J = 17.2 Hz, 1H, CH-3″α), 5.07 (d, J = 10.1 Hz, 1H, CH-3″β), 4.51 (d, J = 8.5 Hz, 1H, CH-7), 3.74 (s, 3H, OCH_3-5), 3.50 (dd, J = 10.2, 6.3 Hz, 1H, CH-8a), 3.47 (s, 3H, OCH_3-6), 3.36 (dd, J = 13.6, 3.1 Hz, 1H, CH-1″α), 3.18 (dd, J = 11.8, 6.5 Hz, 1H, CH-2α), 2.82 (m, 1H, CH-3α), 2.74 (m, 1H, CH-3β), 2.65 (dd, J = 13.6, 8.2 Hz, 1H, CH-1″β), 2.36 (m, 1H, CH-2β), 2.26 (m, 2H, CH_2-8); ^{13}C NMR (125 MHz, $CDCl_3$): δ = 152.7 (C-6a), 144.2 (C-6), 144.0 (C-5), 135.4 (C-1′), 135.3 (CH-2″), 128.4 (CH-3′ and CH-5′), 128.1 (C-3a^1), 127.5 (CH-2′ and CH-6′), 127.1 (C-3a), 126.0 (CH-4′), 117.8 (CH_2-3″), 110.7 (CH-4), 64.4 (CH-8a), 60.3 (OCH_3-6), 58.5 (CH_2-1″), 56.1 (OCH_3-5), 51.0 (CH_2-2), 46.4 (CH-7), 43.8 (CH_2-8), 27.5 (CH_2-3); MS (FAB) m/z (%): 336 $[M+H]^+$, 279 (100), 265 (10); HRESIMS m/z 336.1956 $[M+H]^+$ (336.1964, calc for $C_{22}H_{26}NO_2$).

*4.2.5.3. (E)-6,7-Dimethoxy-2-methyl-1-(prop-1-en-1-yl)-1,2,3,4-tetrahydroisoquinoline (**5d**).*

(*E*)-6,7-Dimethoxy-1-(prop-1-en-1-yl)-1,2,3,4-tetrahydroisoquinoline (**5**) (100 mg, 0.43 mmol) was subjected to similar conditions to those described above to obtain the THIQ **2d** and **3d**. The residue was purified by silica gel column chromatography (CH_2Cl_2/MeOH, 99:1) to afford the compound **5d** (100 mg, 86%) as a yellow oil. ^{1}H NMR (500 MHz, $CDCl_3$): δ = 6.56 (s, 1H, CH-5), 6.54 (s, 1H, CH-8), 5.88 (m, 1H, CH-2″), 5.64 (dt, J = 15.3, 6.3 Hz, 1H, CH-β), 5.44 (dd, J = 15.3, 8.6 Hz, 1H, CH-α), 5.20 (d, J = 17.1 Hz, 1H, CH-3″α), 5.14 (dd, J = 17.1, 10.3 Hz, 1H, CH-3″β), 3.92 (d, J = 8.6 Hz, 1H, CH-1), 3.82 (s, 3H, OCH_3-7), 3.79 (s, 3H, OCH_3-6), 3.42 (m, 1H, CH-1″α), 3.08 (m, 1H, CH-3α), 3.03 (dd, J = 13.8, 7.4 Hz, 1H, CH-1″β), 2.78 (m, 1H, CH-4α), 2.70 (m, 1H, CH-4β), 2.53 (m, 1H, CH-3β), 1.75 (dd, J = 6.3, 1.4 Hz, 3H, CH_3-γ); ^{13}C NMR (125 MHz, $CDCl_3$): δ = 147.5 (C-7), 146.9 (C-6), 135.7 (CH-2″), 132.3 (CH-α), 129.1 (CH-β), 128.9 (C-8a), 126.6 (C-4a), 117.5 (CH_2-3″), 111.2 (CH-8), 111.1 (CH-5), 65.2 (CH-1), 57.5 (CH_2-1″), 56.0 (OCH_3-6), 55.8 (OCH_3-7), 46.1 (CH_2-3), 28.1 (CH_2-4), 17.7 (CH_3-γ); MS (FAB) m/z (%): 274 $[M+H]^+$,

219 (100), 192 (20), 177 (20); HRESIMS *m/z* 274.1806 $[M+H]^+$ (274.1807, calc for $C_{17}H_{24}NO_2$).

4.2.6. General procedure for O-Demethylation

*4.2.6.1. (E)-1-Styryl-1,2,3,4-tetrahydroisoquinoline-6,7-diol (**2a**).*

A solution of the appropriate THIQ **2** (100 mg, 0.34 mmol) in dry CH_2Cl_2 (10 mL) was cooled to −78 °C. To this solution, BBr_3 (0.16 mL, 1.19 mmol) was added dropwise. After 15 min at −78 °C, the reaction mixture was cooled to room temperature and stirred for 2 h. The reaction was finished by the addition of MeOH (1.5 mL) dropwise and the mixture was stirred for another 30 min. The solvent was concentrated to dryness. The residue was purified by silica gel column chromatography (CH_2Cl_2/MeOH, 90:10) to afford the compound **2a** (83 mg, 92%). ^{1}H NMR (500 MHz, CD_3OD): $\delta = 7.40$ (d, $J = 7.7$ Hz, 2H, CH-2′ and CH-6′), 7.28 (t, $J = 7.7$ Hz, 2H, CH-3′ and CH-5′), 7.18 (t, $J = 7.7$ Hz, 1H, CH-4′), 6.55 (d, $J = 15.8$ Hz, 1H, CH-β), 6.52 (s, 1H, CH-8), 6.51 (s, 1H, CH-5), 6.30 (dd, $J = 15.8$, 7.9 Hz, 1H, CH-α), 4.47 (d, $J = 7.9$ Hz, 1H, CH-1), 3.17 (m, 1H, CH-3α), 2.93 (m, 1H, CH-3β), 2.69 (m, 1H, CH-4α), 2.54 (m, 1H, CH-4β); ^{13}C NMR (125 MHz, CD_3OD): $\delta = 144.7$ (C-7), 144.0 (C-6), 138.1 (C-1′), 133.1 (CH-α), 132.4 (CH-β), 129.4 (CH-3′ and CH-5′), 128.5 (C-8a), 128.2 (CH-4′), 127.2 (CH-2′ and CH-6′), 126.8 (C-4a), 116.2 (CH-8), 114.8 (CH-5), 59.8 (CH-1), 42.2 (CH_2-3), 29.2 (CH_2-4); MS (FAB) *m/z* (%): 268 $[M+H]^+$, 251 (100), 173 (20), 123 (30); HRESIMS *m/z* 268.1335 $[M+H]^+$ (268.1338, calc for $C_{17}H_{18}NO_2$).

*4.2.6.2. (E)-2-Methyl-1-styryl-1,2,3,4-tetrahydroisoquinoline-6,7-diol (**2c**).*

(*E*)-6,7-Dimethoxy-2-methyl-1-styryl-1,2,3,4-tetrahydroisoquinoline (**2b**) (100 mg, 0.32 mmol) was subjected to similar conditions to those described above to obtain the THIQ **2a**. The residue was purified by silica gel column chromatography (CH_2Cl_2/MeOH, 90:10) to afford the compound **2c** (82 mg, 91%) as a brown oil. ^{1}H NMR (500 MHz, CD_3OD): $\delta = 7.47$ (d, $J = 7.5$ Hz, 2H, CH-2′ and CH-6′), 7.31 (t, $J = 7.5$ Hz, 2H, CH-3′ and CH-5′), 7.24 (m, 1H, CH-4′), 6.73 (d, $J = 15.8$ Hz, 1H, CH-β), 6.61 (s, 1H, CH-8), 6.56 (s, 1H, CH-5), 6.27 (dd, $J = 15.8$, 8.9 Hz, 1H, CH-α), 4.18 (d, $J = 8.9$ Hz, 1H, CH-1), 3.23 (m, 1H, CH-3α), 3.01 (m, 1H, CH-4α), 2.81 (m, 1H, CH-3β), 2.70 (m, 1H, CH-4β), 2.55 (s, 3H, NCH_3); ^{13}C NMR (125 MHz, CD_3OD): $\delta = 145.2$ (C-7), 144.3 (C-6), 137.3 (C-1′), 135.5 (CH-β), 129.4 (CH-3′ and CH-5′), 129.0 (CH-α), 128.6 (CH-4′), 127.4 (CH-2′ and CH-6′), 126.1 (C-8a), 125.0 (C-4a), 115.7 (CH-8), 115.1 (CH-5), 68.5 (CH-1), 51.4 (CH_2-3), 43.1 (NCH_3), 27.7 (CH_2-4); MS (FAB) *m/z* (%): 282 $[M+H]^+$, 251 (100), 178 (70), 173 (100), 123 (90); HRESIMS *m/z* 282.1487 $[M+H]^+$ (282.1494, calc for $C_{18}H_{20}NO_2$).

*4.2.6.3. (E)-2-Allyl-1-styryl-1,2,3,4-tetrahydroisoquinoline-6,7-diol (**2e**).*

(*E*)-2-Allyl-6,7-dimethoxy-1-styryl-1,2,3,4-tetrahydroisoquinoline (**2d**) (100 mg, 0.29 mmol) was subjected to similar conditions to those described above to obtain the THIQ **2a** and **2c**. The residue was purified by silica gel column chromatography (CH_2Cl_2/MeOH, 90:10) to afford the compound **2e** (85 mg, 93%) as a brown oil. ^{1}H NMR (500 MHz, CD_3OD): $\delta = 7.24$ (d, $J = 7.2$ Hz, 2H, CH-2′ and CH-6′), 7.19 (t, $J = 7.2$ Hz 2H, CH-3′ and CH-5′), 7.13 (m, 1H, CH-4′), 6.39 (d, $J = 15.8$ Hz, 1H, CH-β), 6.37 (s, 1H, CH-8), 6.22 (s, 1H, CH-5), 6.06 (dd, $J = 15.8$, 8.9 Hz, 1H, CH-α), 5.86 (m, 1H, CH-2″), 5.12 (m, 2H, CH_2-3″), 3.99 (d, $J = 8.9$ Hz, 1H, CH-1), 3.39 (dd, $J = 13.6$, 5.6 Hz, 1H, CH-1″α), 3.02 (m, 1H, CH-3α), 2.99 (m, 1H, CH-1″β), 2.59 (m, 1H, CH-4α), 2.48 (m, 1H, CH-4β), 2.47 (m, 1H, CH-3β); ^{13}C NMR (125 MHz, CD_3OD): $\delta = 143.5$ (C-7), 143.0 (C-6), 136.3 (C-1′), 134.5 (CH-β), 133.4 (CH-2″), 128.6 (CH-3′ and CH-5′), 128.5 (CH-α), 127.8 (CH-4′), 126.9 (C-8a), 126.5 (CH-2′ and CH-6′), 125.5 (C-4a), 119.7 (CH_2-3″), 115.0 (CH-8), 114.5 (CH-5), 65.6 (CH-1), 57.9 (CH_2-1″), 46.4 (CH_2-3), 27.4 (CH_2-4); MS (FAB) *m/z* (%): 308 $[M+H]^+$, 253 (50), 161 (30), 123 (100); HRESIMS *m/z* 308.1637 $[M+H]^+$ (308.1651, calc for $C_{20}H_{22}NO_2$).

*4.2.6.4. 7-Phenyl-1,2,3,7,8,8a-hexahydrocyclopenta[ij]isoquinoline-5,6-diol (**3a**).*

5,6-Dimethoxy-7-phenyl-1,2,3,7,8,8a-hexahydrocyclopenta[*ij*]isoquinoline (**3**) (100 mg, 0.34 mmol) was subjected to similar conditions to those described above to obtain the THIQ **2a**, **2c** and **2e**. The residue was purified by silica gel column chromatography (CH_2Cl_2/MeOH, 90:10) to afford the compound **3a** (77 mg, 88%) as a brown oil. ^{1}H NMR and HRESIMS [19]; ^{13}C NMR (125 MHz, CD_3OD): $\delta = 147.7$ (C-6a), 143.5 (C-6), 141.8 (C-5), 129.5 (C-1′), 129.2 (CH-3′ and CH5′), 128.9 (C-3a^1), 128.2 (CH-2′ and CH-6′), 127.2 (CH-4′), 121.6 (C-3a), 114.2 (CH-4), 58.1 (CH-8a), 46.4 (CH-7), 44.4 (CH_2-2), 42.5 (CH_2-8), 23.6 (CH_2-3); MS (FAB) *m/z* (%): 268 $[M+H]^+$, 251 (100), 239 (80), 190 (30), 154 (50).

*4.2.6.5. 1-Methyl-7-phenyl-1,2,3,7,8,8a-hexahydrocyclopenta[ij]isoquinoline-5,6-diol (**3c**).*

5,6-Dimethoxy-1-methyl-7-phenyl-1,2,3,7,8,8a-hexahydrocyclopenta[*ij*]isoquinoline (**3d**) (100 mg, 0.32 mmol) was subjected to similar conditions to those described above to obtain THIQ **2a**, **2c**, **2e** and **3a**. The residue was purified by silica gel column chromatography (CH_2Cl_2/MeOH, 90:10) to afford compound **3c** (84 mg, 94%) as a green oil [19]. ^{1}H NMR (500 MHz, CD_3OD): $\delta = 7.26$ (t, $J = 7.5$ Hz, 2H, CH-3′ and CH-5′), 7.16 (m, 2H, CH-2′ and CH-6′), 7.14 (m, 1H, CH-4′), 6.48 (s, 1H, CH-4), 4.42 (d, $J = 8.4$ Hz, 1H, CH-7), 3.38 (m, 1H, CH-8a), 3.07 (m, 1H, CH-2α), 2.72 (m, 1H, CH-3α), 2.63 (m, 1H, CH-3β), 2.49 (m, 1H, CH-2β), 2.36 (m, 1H, CH-8α), 2.20 (s, 1H, NCH_3), 2.14 (m, 1H, CH-8β); ^{13}C NMR (125 MHz, CD_3OD): $\delta = 145.4$ (C-6), 143.7 (C-5), 140.1 (C-6a), 128.5 (C-1′), 128.1 (CH-3′ and CH-5′), 128.0 (C-3a^1), 127.2 (CH-2′ and CH-6′), 125.8 (CH-4′), 121.1 (C-3a), 112.9 (CH-4), 65.6 (CH-8a), 54.4 (CH_2-2), 45.1 (CH-7), 42.7 (CH_2-8), 39.9 (NCH_3), 26.0 (CH_2-3); MS (FAB) *m/z* (%): 282 $[M+H]^+$, 265 (50), 253 (65), 239 (100), 175 (20); HRESIMS *m/z* 282.1495 $[M+H]^+$ (282.1494, calc for $C_{18}H_{20}NO_2$).

*4.2.6.6. 1-Allyl-7-phenyl-1,2,3,7,8,8a-hexahydrocyclopenta[ij]isoquinoline-5,6-diol (**3e**).*

1-Allyl-5,6-dimethoxy-7-phenyl-1,2,3,7,8,8a-hexahydrocyclopenta[*ij*]isoquinoline (**3d**) (100 mg, 0.29 mmol) was subjected to similar conditions to those described above to obtain THIQ **2a**, **2c**, **2e**, **3a** and **3c**. The residue was purified by silica gel column chromatography (CH_2Cl_2/MeOH, 90:10) to afford the compound **3e** (82 mg, 90%) as a brown oil. ^{1}H NMR and HRESIMS [19]; ^{13}C NMR (125 MHz, CD_3OD): $\delta = 145.7$ (C-6), 144.9 (C-5), 140.8 (C-6a), 136.7 (CH-2″), 135.4 (C-1′), 129.2 (C-3a^1), 128.9 (CH-3′ and CH-5′), 128.4 (CH-2′ and CH-6′), 126.7 (CH-4′), 123.5 (C-3a), 117.6 (CH_2-3″),113.6 (CH-4), 65.5 (CH-8a), 59.2 (CH_2-1″), 52.2 (CH_2-2), 46.6 (CH-7), 44.7 (CH_2-8), 27.8 (CH_2-3); MS (FAB) *m/z* (%): 308 $[M+H]^+$, 251 (100), 175 (10).

*4.2.6.7. (E)-1-(prop-1-en-1-yl)-1,2,3,4-tetrahydroisoquinoline-6,7-diol (**5a**).*

(*E*)-6,7-Dimethoxy-1-(prop-1-en-1-yl)-1,2,3,4-tetrahydroisoquinoline (**5**) (100 mg, 0.43 mmol) was subjected to similar conditions to those described above to obtain THIQ **2a**, **2c**, **2e**, **3a**, **3c** and **3e**. The residue was purified by silica gel column chromatography (CH_2Cl_2/MeOH, 90:10) to afford compound **5a** (78 mg, 89%) as a brown oil. ^{1}H NMR (500 MHz, CD_3OD): $\delta = 6.61$ (s, 1H, CH-5), 6.54 (s, 1H, CH-8), 6.03 (dq, $J = 13.2$, 6.6 Hz, 1H, CH-β), 5.60 (ddd, $J = 15.2$, 8.4, 1.6 Hz, 1H, CH-α), 4.35 (m, 1H, CH-1), 3.48 (m, 1H, CH-3α), 3.33 (m, 1H, CH-3β), 2.99 (m, 1H, H-4α), 2.89 (dd, $J = 17.0$, 5.3 Hz, 1H, H-4β), 1.83 (dd, $J = 6.5$, 1.3 Hz, 3H, CH_3-γ); ^{13}C NMR (125 MHz, CD_3OD): $\delta = 146.8$ (C-7), 145.7 (C-6), 137.0 (CH-β), 127.9 (CH-α), 123.8 (C-8a), 123.3 (C-4a), 116.1 (CH-8), 114.8 (CH-5),

59.1 (CH-1), 41.3 (CH_2-3), 25.8 (CH_2-4), 18.0 (CH_3-γ); MS (FAB) *m/z* (%): 206 $[M+H]^+$, 191 (35), 189 (100), 161 (55); HRESIMS *m/z* 206.1177 $[M+H]^+$ (206.1181, calc for $C_{12}H_{16}NO_2$).

*4.2.6.8. (E)-2-Methyl-1-(prop-1-en-1-yl)-1,2,3,4-tetrahydroisoquinoline-6,7-diol (**5c**).*

(*E*)-6,7-Dimethoxy-2-methyl-1-(prop-1-en-1-yl)-1,2,3,4-tetrahydroisoquinoline (**5b**) (100 mg, 0.40 mmol) was subjected to similar conditions to those described above to obtain THIQ **2a**, **2c**, **2e**, **3a**, **3c**, **3e** and **5a**. The residue was purified by silica gel column chromatography (CH_2Cl_2/MeOH, 90:10) to afford the compound **5c** (81 mg, 92%) as a brown oil. ^{1}H NMR (500 MHz, CD_3OD): $\delta = 6.58$ (s, 1H, CH-5), 6.51 (s, 1H, CH-8), 5.98 (dq, $J = 13.4$, 6.2 Hz, 1H, CH-β), 5.47 (dd, $J = 13.4$, 8.8, Hz, 1H, CH-α), 4.39 (d, $J = 8.8$ Hz, 1H, CH-1), 3.43 (m, 1H, CH-3α), 3.10 (ddd, $J = 14.2$, 9.6, 5.2 Hz, 1H, CH-3β), 3.00 (dd, $J = 9.6$, 5.8 Hz, 1H, CH-4α), 2.85 (dt, $J = 17.0$, 5.2 Hz, 1H, CH-4β), 2.72 (s, 3H, NCH_3), 1.84 (dd, $J = 6.2$, 1.6 Hz, 3H, CH_3-γ); ^{13}C NMR (125 MHz, CD_3OD): $\delta = 146.5$ (C-7), 145.5 (C-6), 136.6 (CH-β), 128.2 (CH-α), 124.6 (C-8a), 123.7 (C-4a), 115.9 (CH-8), 115.2 (CH-5), 68.7 (CH-1), 51.4 (CH_2-3), 41.9 (NCH_3), 26.7 (CH_2-4), 18.0 (CH_3-γ); MS (FAB) *m/z* (%): 220 $[M+H]^+$, 189 (100), 178 (20), 151 (45), 149 (20); HRESIMS *m/z* 220.1332 $[M+H]^+$ (220.1338, calc for $C_{13}H_{18}NO_2$).

*4.2.6.9. (E)-2-Allyl-1-(prop-1-en-1-yl)-1,2,3,4-tetrahydroisoquinoline-6,7-diol (**5e**).*

(*E*)-2-Allyl-6,7-dimethoxy-1-(prop-1-en-1-yl)-1,2,3,4-tetrahydroisoquinoline (**5d**) (100 mg, 0.37 mmol) was subjected to similar conditions to those described above to obtain THIQ **2a**, **2c**, **2e**, **3a**, **3c**, **3e**, **5a** and **5c**. The residue was purified by silica gel column chromatography (CH_2Cl_2/MeOH, 90:10) to afford the compound **5e** (84 mg, 94%) as a brown oil. ^{1}H NMR (500 MHz, CD_3OD): $\delta = 6.52$ (s, 1H, CH-5), 6.49 (s, 1H, CH-8), 5.93 (m, 1H, CH-2″), 5.76 (m, 1H, CH-β), 5.44 (m, 1H, CH-α), 5.39 (m, 1H, CH-3″α), 5.29 (m, 1H, CH-3″β), 4.10 (d, $J = 8.9$ Hz, 1H, CH-1), 3.56 (m, 1H, CH-1″), 3.19 (m, 1H, CH-3α), 3.14 (m, 1H, CH-1″β), 2.73 (m, 1H, CH-4α), 2.69 (m, 1H, CH-4β), 2.67 (m, 1H, CH-3β), 1.79 (dd, $J = 6.5$, 1.6 Hz, 3H, CH_3-γ); ^{13}C NMR (125 MHz, CD_3OD): $\delta = 145.9$ (C-7), 145.0 (C-6), 133.6 (CH-2″), 133.2 (CH-β), 131.1 (CH-α), 127.2 (C-8a), 125.4 (C-4a), 121.2 (CH_2-3″), 115.7 (CH-8), 115.5 (CH-5), 66.8 (CH-1), 58.2 (CH_2-1″), 47.7 (CH_2-3), 27.8 (CH_2-4), 17.9 (CH_3-γ); MS (FAB) *m/z* (%): 246 $[M+H]^+$, 191 (100), 161 (10), 149 (25); HRESIMS *m/z* 246.1498 $[M+H]^+$ (246.1494, calc for $C_{15}H_{20}NO_2$).

4.3. Biological assays

All research with human samples in this study, were complied with the principles of the *Declaration of Helsinki* and was approved by the institutional ethics committee of the University Clinic Hospital of Valencia (Valencia, Spain). Written, informed consent was obtained from volunteers.

4.3.1. Cell culture

Human umbilical venous endothelial cells (HUVEC) were isolated by collagenase treatment [42] and maintained in human specific endothelial basal medium (EBM-2) supplemented with endothelial growth media (EGM-2) and 10% FBS. Cells up to passage one were grown to confluence on 24-well culture plates. Prior to every experiment, cells were incubated 16 h in medium containing 1% FBS and returned at the beginning of experimental protocols to the 10% FBS medium.

4.3.2. Binding assays

Binding experiments were performed on striatal membranes. Each striatum was homogenized in 2 mL ice-cold Tris-HCl buffer (50 mM, pH = 7.4 at 22 °C) with a Polytron (4s, maximal scale) and immediately diluted with Tris buffer. The homogenate was centrifuged either twice ([^{3}H] SCH 23390 binding experiments) or four times ([^{3}H] raclopride binding experiments) at 20000 g for 10 min at 4 °C with resuspension in the same volume of Tris buffer between centrifugations. For [^{3}H] SCH 23390 binding experiments, the final pellet was resuspended in Tris buffer containing 5 mM $MgSO_4$, 0.5 mM EDTA and 0.02% ascorbic acid (Tris-Mg buffer), and the suspension was briefly sonicated and diluted to a protein concentration of 1 mg/mL. An aliquot of 100 μL of freshly prepared membrane suspension (100 μg of striatal protein) was incubated for 1 h at 25 °C with 100 μL Tris buffer containing [^{3}H] SCH 23390 (0.25 nM final concentration) and 800 μL of Tris-Mg buffer containing the required drugs. Non-specific binding was determined in the presence of 30 μM SK&F 38393 and represented around 2–3% of total binding. For [^{3}H] raclopride binding experiments, the final pellet was resuspended in Tris buffer containing 120 mM NaCl, 5 mM KCl, 1 mM $CaCl_2$, 1 mM $MgCl_2$ and 0.1% ascorbic acid (Tris-ions buffer), and the suspension was treated as described above. A 200 μL aliquot of freshly prepared membrane suspension (200 μg of striatal protein) was incubated for 1 h at 25 °C with 200 μL of Tris buffer containing [^{3}H] raclopride (0.5 nM final concentration) and 400 μL of Tris-ions buffer containing the drug being investigated. Non-specific binding was determined in the presence of 50 μM apomorphine and represented around 5–7% of total binding. In both cases, incubations were stopped by addition of 3 mL of ice-cold buffer (Tris-Mg buffer or Tris-ions buffer, as appropriate) followed by rapid filtration through Whatman GF/B filters using a Brandel harvester (model M – 24, Biochemical Research and Development Laboratories, Inc.). Tubes were rinsed with 3 mL ice-cold buffer, and filters were washed with 3 × 3 mL ice-cold buffer. After the filters had been dried, radioactivity was counted in 4 mL scintillation liquid (Optiphase 'Hisafe' 2, Perkin Elmer). Filter blanks corresponded to approximately 0.5% of total binding and were not modified by drugs.

4.3.3. Cytotoxicity studies

The cytotoxity of **2c**, **2e**, **3a**, **3c**, **3e**, **5c** and **5e** was determined at 30 μM on neutrophils and HUVEC by the use of two different approaches: the MTT colorimetric assay and flow cytometry analysis of cell apoptosis and survival [43].

4.3.4. MTT assay

The viability of neutrophils and HUVEC was determined using the previously described MTT (3[4,5-dimethylthiazol-2-yl]-2,5-diphenyltetrazolium bromide) colorimetric assay [44]. Neutrophils were obtained from buffy coats of healthy donors by Ficoll-Hypaque density gradient centrifugation as described [45]. Neutrophils and HUVEC suspension in supplemented RPMI medium (10^5 cells/100 μL) was added to each well of a 96-well microtiter plate. Cells were incubated in the absence or presence of the compounds at 37 °C for 24 h. MTT was freshly prepared at 2 mg/mL in PBS. 100 μL of MTT solution was added to each well and incubated at 37 °C for another 3 h. The supernatants were discarded and 200 μL of DMSO was added to each well to dissolve formazan. The optical densities at dual wavelengths (560 and 630 nm) were determined in a spectrophotometer (Infinite M200, Tecan, Mannedorf, Switzerland).

4.3.4.1. Cytofluorometric analysis of apoptosis and survival. Freshly isolated neutrophils and HUVEC were resuspended in supplemented RPMI medium at 2 × 10^6 cells/mL. 25 μL and cultured in a 96-well plate containing 200 μL of supplemented RPMI medium for 24 h in the absence or presence of the compounds as described previously [46]. Assessment of apoptosis was performed by flow cytometry using annexin V-FITC and propidium

iodide (PI). The protocol indicated by the manufacturer (FITC Annexin V Apoptosis Detection Kit I; BD Biosciences) was used as outlined previously [47]. Cells (1×10^4) were analyzed in a BD FACSVerse Flow Cytometer (BD Biosciences, San Jose, CA) and differentiated as early or viable apoptotic (annexin V^+ and PI^-), late apoptotic and/or necrotic (annexin V^+ and PI^+), and viable non-apoptotic (annexin V^- and PI^-) cells.

4.4. Molecular modeling

4.4.1. Set up of dopaminergic receptors D_1 and D_2

3D models of the human D_1 and D_2 DRs were used for the molecular modeling study. Both models are based on the homology model from the crystallized D3 DR, β_2 adrenoceptor and $A_{2\alpha}$ adenosine receptor as templates [48]. These models were successfully used previously to perform molecular modeling studies of different dopamine receptor ligands [14,15,17,18,32,33].

4.4.2. Molecular docking

AutoDock 4 [30] was used to dock each compound to the receptor active site using a Lamarckian genetic algorithm with pseudo-Solis and Wets local search [49]. The following parameters were used: the initial population of trial ligands was constituted by 250 individuals; the maximum number of generations was set to 2.7 × 104. The maximum number of energy evaluations was 10.0 × 106. For each docking job, 100 conformations were generated. All other run parameters were maintained at their default setting. The resulting docked conformations were clustered into families by considering the backbone rmsd. The lowest docking-energy conformation was considered the most favorable orientation [50].

4.4.3. MD simulations

The complex geometries from docking were soaked in boxes of explicit water using the TIP3P model [51] and subjected to MD simulation. All MD simulations were performed with the Amber software package [31] using periodic boundary conditions and cubic simulation cells. The particle mesh Ewald method (PME) [52] was applied using a grid spacing of 1.2 Å, a spline interpolation order of 4 and a real space direct sum cutoff of 10 Å. The SHAKE algorithm was applied allowing for an integration time step of 2 fs. MD simulations were carried out at 310 K temperature. Three MD simulations of 3 ns were conducted for each system under different starting velocity distribution functions; thus, in total 9 ns were simulated for each complex. The NPT ensemble was employed using Berendsen coupling to a baro/thermostat (target pressure 1 atm, relaxation time 0.1 ps). Post MD analysis was carried out with program PTRAJ.

4.4.4. QM/MM setup

The most important question when using the ONIOM scheme is the partitioning of the system into high and low level layers. In this study, the binding site of the receptor residues was identified by the use of the free energy decomposition approach (MM/GBSA). The side chains of the binding site residues that contributed with a $|\Delta G|$ higher than 1.0 kcal/mol in the per residue energy decomposition together with each inhibitor were included at the high-level QM layer, and the remainder of the complex system was included in the low-level MM layer. The QM region was calculated using the M062X/6-31G(d) method [53] and the MM portion by the use of the AMBER force field [54]. The MM parameters absent in the standard AMBER force field were included from the generalized amber force field (GAFF) [55]. Only the geometry of the QM layer was fully optimized. Hydrogen link atoms were used to satisfy atoms at the QM and MM interface. The hydrogen link atoms remained fixed during optimization.

4.4.5. Atoms in molecules theory

After the QM/MM calculation, the optimized geometry for each complex was used as input for quantum theory atoms in molecule (QTAIM) analysis [33], which was performed with the help of Multiwfn software [56], using the wave functions generated at the M062X-D/6-31G(d) level. This type of calculations have been used in recent studies since it ensures a reasonable compromise between the wave function quality required to obtain reliable values of the derivatives of $\rho(r)$ and the computer power available, which is due to the extension of the system in study [57,58].

4.4.6. Additional materials

FITC-Annexin and propidium iodide staining solution were from BD Bioscience (San Jose, CA). Unless stated, all other reagents were from Sigma-Aldrich.

Acknowledgements

This study was supported by grants SAF2014-57845-R from the Spanish Ministry of Economy and Competiveness, the European Regional Development Fund (FEDER) and research grants from Generalitat Valenciana (PROMETEO II/2013/014). This study was also supported by the Spanish Ministry of Economy and Competitiveness through a Miguel Servet Program (CP15/00150) ISCIII (Carlos III Institute of Health) co-funded by the European Regional Development Fund (FEDER)/European Social Fund (ESF). Grants from the Universidad Nacional de San Luis (UNSL-Argentina) partially supported this work. R.D.E. and SAA are members of the Consejo Nacional de Investigaciones Científicas y Técnicas (CONICET-Argentina) staff and L.J.G acknowledges to CONICET-Argentina by a postdoctoral fellowship. The authors would like to thanks MSc. Daniel O. Zamo for technical assistance (CONICET-Argentina).

Appendix A. Supplementary data

Supplementary data related to this article can be found at http://dx.doi.org/10.1016/j.ejmech.2016.06.009.

References

[1] M.F. Roberts, M. Wink, Alkaloids: Biochemistry, Ecology, and Medicinal Applications, Plenum Press, New York, 1998.
[2] J.D. Phillipson, M.F. Roberts, M.H. Zenk, The Chemistry and Biology of Isoquinoline Alkaloids, Springer-Verlag, Berlin, 1985.
[3] J.D. Scott, R.M. Williams, Chemistry and biology of the tetrahydroisoquinoline antitumor antibiotics, Chem. Rev. 102 (2002) 1669–1730.
[4] V.I. Nikulin, I.M. Rakov, J.E. De Los Angeles, R.C. Metha, L.Y. Boyd, D.R. Feller, D.D. Miller, 1-Benzyl-1,2,3,4-tetrahydroisoquinoline-6,7-diols as novel affinity and photoaffinity probes for β-adrenoceptor subtypes, Bioorg. Med. Chem. 14 (2006) 1684–1697.
[5] K. Takada, T. Uehara, Y. Nakao, S. Matsunaga, R.W. Van Soest, N.J. Fusetani, Schulzeines A–C, new α-glucosidase inhibitors from the marine sponge *Penares schulzei*, J. Am. Chem. Soc. 126 (2004) 187–193.
[6] M. Ludwig, C.E. Hoesl, G. Höfner, K.T. Wanner, Affinity of 1-aryl-1,2,3,4-tetrahydroisoquinoline derivatives to the ion channel binding site of the NMDA receptor complex, Eur. J. Med. Chem. 41 (2006) 1003–1010.
[7] A. Bermejo, P. Protais, M.A. Blázquez, K.S. Rao, M.C. Zafra-Polo, D. Cortes, Dopaminergic isoquinoline alkaloids from roots of *Xylopia papuana*, Nat. Prod. Lett. 6 (1995) 57–62.
[8] P. Protais, J. Arbaoui, E.H. Bakkali, A. Bermejo, D. Cortes, Effects of various isoquinoline alkaloids on *in vitro* ^{3}H-dopamine uptake, J. Nat. Prod. 58 (1995) 1475–1484.
[9] N. Cabedo, P. Protais, B.K. Cassels, D. Cortes, Synthesis and dopamine receptor selectivity of the benzyltetrahydroisoquinoline, (*R*)-(+)-*nor*-roefractine, J. Nat. Prod. 61 (1998) 709–712.
[10] I. Andreu, D. Cortes, P. Protais, B.K. Cassels, A. Chagraoui, N. Cabedo, Preparation of dopaminergic *N*-alkyl-benzyltetrahydroisoquinolines using a 'one-pot' procedure in acid medium, Bioorg. Med. Chem. 8 (2000) 889–895.
[11] N. Cabedo, I. Andreu, M.C. Ramírez de Arellano, A. Chagraoui, A. Serrano, A. Bermejo, P. Protais, D. Cortes, Enantioselective syntheses of dopaminergic

(*R*)- and (*S*)-benzyltetrahydroisoquinolines, J. Med. Chem. 44 (2001) 1794–1801.
[12] I. Andreu, N. Cabedo, G. Torres, A. Chagraoui, M.C. Ramirez de Arellano, S. Gil, A. Bermejo, M. Valpuesta, P. Protais, D. Cortes, Syntheses of dopaminergic 1-cyclohexylmethyl-7,8-dioxygenated tetrahydroisoquinolines by selective heterogeneous tandem hydrogenation, Tetrahedron 58 (2002) 10173–10179.
[13] F.D. Suvire, N. Cabedo, A. Chagraoui, M.A. Zamora, D. Cortes, R.D. Enriz, Molecular recognition and binding mechanism of *N*-alkyl-benzyltetrahydroisoquinolines to the D_1 dopamine receptor. A computational approach, J. Mol. Struc. (Teochem) 666–667 (2003) 455–467.
[14] I. Berenguer, N. El Aouad, S. Andujar, V. Romero, F. Surive, T. Freret, A. Bermejo, M.D. Ivorra, R.D. Enriz, M. Boulouard, N. Cabedo, D. Cortes, Tetrahydroisoquinolines as dopaminergic ligands: 1-butyl-7-chloro-6-hydroxy-tetrahydroisoquinoline, a new compound with antidepressant-like activity in mice, Bioorg. Med. Chem. 17 (2009) 4968–4980.
[15] N. El Aouad, I. Berenguer, V. Romero, P. Marín, A. Serrano, S. Andujar, F. Suvire, A. Bermejo, M.D. Ivorra, R.D. Enriz, N. Cabedo, D. Cortes, Structure-activity relationship of dopaminergic halogenated 1-benzyl-tetrahydroisoquinoline derivatives, Eur. J. Med. Chem. 44 (2009) 4616–4621.
[16] N. Cabedo, I. Berenguer, B. Figadère, D. Cortes, An overview on benzylisoquinoline derivatives with dopaminergic and serotonergic activities, Curr. Med. Chem. 16 (2009) 2441–2467.
[17] S.A. Andujar, R.D. Tosso, F.D. Suvire, E. Angelina, N. Peruchena, N. Cabedo, D. Cortes, R.D. Enriz, Searching the biologically relevant conformation of dopamine: a computational approach, J. Chem. Inf. Model 52 (2012) 99–112.
[18] S. Andujar, F. Suvire, I. Berenguer, N. Cabedo, P. Marín, L. Moreno, M.D. Ivorra, D. Cortes, R.D. Enriz, Tetrahydroisoquinolines acting as dopaminergic ligands. A molecular modeling study using MD simulations and QM calculations, J. Mol. Model 18 (2012) 419–431.
[19] J. Párraga, A. Galán, M.J. Sanz, N. Cabedo, D. Cortes, Synthesis of hexahydrocyclopenta[*ij*]isoquinolines as a new class of dopaminergic agents, Eur. J. Med. Chem. 90 (2015) 101–106.
[20] W. Poewe, Treatments for Parkinson disease-past achievements and current clinical needs, Neurology 72 (2009) S65–S73.
[21] J.M. Beaulieu, R.R. Gainetdinov, The Physiology, signaling, and pharmacology of dopamine receptors, Pharmacol. Rev. 63 (2011) 182–217.
[22] N. Clausius, C. Born, H. Grunze, The relevance of dopamine agonists in the treatment of depression, Neuropsychiatry 23 (2009) 15–25.
[23] A.A. Gershon, T. Vishne, L. Grunhaus, Dopamine D_2-like receptors and the antidepressant response, Biol. Psychiatry 61 (2007) 145–153.
[24] A.M. Basso, K.B. Gallagher, N.A. Bratcher, J.D. Brioni, R.B. Moreland, G.C. Hsieh, K. Drescher, G.B. Fox, M.W. Decker, L.E. Rueter, Antidepressant-like effect of D(2/3) receptor-, but not D(4) receptor-activation in the rat forced swim test, Neuropsychopharmacology 30 (2005) 1257–1268.
[25] E.P. Eaton, G.R. Carlson, J.T. Lee, Phosphorus pentoxide-methanesulfonic acid, Convenient alternative to polyphosphoric acid, J. Org. Chem. 38 (1972) 4071–4073.
[26] D. Ghosh, S.E. Snyder, V.J. Watts, R.B. Mailman, D.E. Nichols, 8,9-Dihydroxy-2,3,7,11b-tetrahydro-1H-naph[1,2,3-de]isoquinoline: a potent full dopamine D1 agonist containing a rigid β-phenyldopamine pharmacophore, J. Med. Chem. 39 (1996) 549–555.
[27] N. Ye, J.L. Neumeyer, R.J. Baldessarini, X. Zhen, A. Zhang, Update 1 of: recent progress in development of dopamine receptor subtype-selective agents: potential therapeutics for neurological and psychiatric disorders, Chem. Rev. 113 (2013) 123–178.
[28] Y. Ito, S. Horie, Y. Shindo, A Novel [2+2] photodimerization of N-[(E)-3,4-methylenedioxycinnamoyl]dopamine in the solid state, Org. Lett. 3 (2001) 2411–2413.
[29] A.P. Dwivedi, S. Kumar, V. Varshney, A.B. Singh, A.K. Srivastava, D.P. Sahu, Synthesis and antihyperglycemic activity of novel N-acyl-2-arylethylamines and N-acyl-3-coumarylamines, Bioorg. Med. Chem. Lett. 18 (2008) 2301–2305.
[30] G.M. Morris, R. Huey, W. Lindstrom, M.F. Sanner, R.K. Belew, D.S. Goodsell, A.J. Olson, Autodock4 and autodocktools4: automated docking with selective receptor flexibility, J. Comput. Chem. 16 (2009) 2785–2791.
[31] D.A. Case, T.E. Cheatham, T. Darden, H. Gohlke, R. Luo, K.M. Merz Jr., A. Onufriev, C. Simmerling, B. Wang, R.J. Woods, The Amber biomolecular simulation programs, J. Comput. Chem. 26 (2005) 1668–1688.
[32] V.-H. Esteban, R.D. Tosso, R.D. Enriz, L.J. Gutierrez, Molecular insight into the interaction mechanisms of inhibitors (R)-1t and (S)-1m with BACE1 protease: QM/MM Investigations, Int. J. Quantum Chem. 115 (2015) 389–397.
[33] R.F.W. Bader, Atoms in molecules, Acc. Chem. Res. 18 (1985) 9–15.
[34] E.L. Angelina, S.A. Andujar, R.D. Tosso, R.D. Enriz, N.M. Peruchena, Non-covalent interactions in receptor-ligand complexes. A study based on the electron charge density, J. Phys. Org. Chem. 27 (2014) 128–134.
[35] J. Párraga, N. Cabedo, S. Andujar, L. Piqueras, L. Moreno, A. Galán, E. Angelina, R.D. Enriz, M.D. Ivorra, M.J. Sanz, D. Cortes, 2,3,9- and 2,3,11-Trisubstituted tetrahydroprotoberberines as D2 dopaminergic ligands, Eur. J. Med. Chem. 68 (2013) 150–166.
[36] P. Nagy, G. Alagona, C. Ghio, Theoretical studies on the conformation of protonated dopamine in the gas phase and in aqueous solution, J. Am. Chem. Soc. 121 (1999) 4804–4815.
[37] H. Berendsen, D. Van der Spoel, R. Van Drunen, GROMACS: a message-passing parallel molecular dynamics implementations, Comput. Phys. Commun. 91 (1995) 43–56.
[38] Y.T. Wang, Z.-Y. Su, C.-H. Hsieh, C.-L. Chen, Predictions of binding for dopamine D_2 receptor antagonists by the SIE method, J. Chem. Inf. Model 49 (2009) 2369–2375.
[39] R.D. Tosso, S.A. Andujar, L. Gutierrez, E. Angelina, R. Rodríguez, M. Nogueras, H. Baldoni, F.D. Suvire, J. Cobo, R.D. Enriz, Molecular modeling study of dihydrofolate reductase inhibitors. Molecular dynamics simulations, quantum mechanical calculations, and experimental corroboration, J. Chem. Inf. Model 53 (2013) 2018–2032.
[40] H. Lan, C.J. DuRand, M.M. Teeter, K.A. Neve, Structural determinants of pharmacological specificity between D_1 and D_2 dopamine receptors, Mol. Pharmacol. 69 (2006) 185–194.
[41] K.A. Neve, M.G. Cumbay, K.R. Thompson, R. Yang, D.C. Buck, V.J. Watts, C.J. Durand, M.M. Teeter, Mol. Pharmacol. 60 (2001) 373–381.
[42] E.A. Jaffe, R.L. Nachman, C.G. Becker, C.R. Minick, Culture of human endothelial cells derived from umbilical veins. Identification by morphologic and immunologic criteria, J. Clin. Invest 52 (1973) 2745–2756.
[43] L.E. Smith, S. Rimmer, S. MacNeil, Examination of the effects of poly(*N*-vinyl pyrrolidinone) hydrogels in direct and indirect contact with cells, Biomaterials 27 (2006) 2806–2812.
[44] M. Iacobini, A. Menichelli, G. Palumbo, G. Multari, B. Werner, D. Del Principe, Involvement of oxygen radicals in cytarabineinduced apoptosis in human polymorphonuclear cells, Biochem. Pharmacol. 61 (2001) 1033–1040.
[45] T. Mateo, Y. Naim Abu Nabah, M. Losada, R. Estelles, C. Company, B. Bedrina, J.M. Cerda-Nicolas, S. Poole, P.J. Jose, J. Cortijo, E.J. Morcillo, M.J. Sanz, A critical role for TNFalpha in the selective attachment of mononuclear leukocytes to angiotensin-II-stimulated arterioles, Blood 110 (2007) 1895–1902.
[46] M.T. García, M.A. Blázquez, M.J. Ferrándiz, M.J. Sanz, N. Silva-Martín, J.A. Hermoso, A.G. de la Campa, New alkaloid antibiotics that target the DNA topoisomerase I of *Streptococcus pneumonia*, J. Biol. Chem. 286 (2011) 6402–6413.
[47] M.C. Martin, I. Dransfield, C. Haslett, A.G. Rossi, Cyclic AMP regulation of neutrophil apoptosis occurs via a novel protein kinase A-independent signaling pathway, J. Biol. Chem. 276 (2001) 45041–45050.
[48] M.A. Soriano-Ursua, J.O. Ocampo-Lopez, K. Ocampo-Mendoza, J.G. Trujillo-Ferrara, J. Correa-Basurto, Theoretical study of 3-D molecular similarity and ligand binding modes of orthologous human and rat D_2 dopamine receptors, Comput. Biol. Med. 41 (2011) 537–545.
[49] G.M. Morris, D.S. Goodsell, R.S. Halliday, R. Huey, W.E. Hart, R.K. Belew, A.J. Olson, Automated docking using a Lamarckian genetic algorithm and an empirical binding free energy function, J. Comput. Chem. 19 (1998) 1639–1662.
[50] T.J.A. Ewing, I.D. Kuntz, Critical evaluation of search algorithms for automated molecular docking and database screening, J. Comput. Chem. 18 (1997) 1175–1189.
[51] W.L. Jorgensen, J. Chandrasekhar, J.D. Madura, R.W. Impey, M.L. Klein, Comparison of simple potential functions for simulating liquid water, J. Chem. Phys. 79 (1983) 926–935.
[52] T. Darden, D. York, L. Pedersen, Particle mesh Ewald: an N, log (N) method for Ewald sums in large systems, J. Chem. Phys. 98 (1993) 10089–10092.
[53] Y. Zhao, D.G. Truhlar, The M06 suite of density functionals for main group thermochemistry, thermochemical kinetics, noncovalent interactions, excited states, and transition elements: two new functionals and systematic testing of four M06-class functionals and 12 other functionals, Theor. Chem. Acc. 120 (2008) 215–241.
[54] W.D. Cornell, P. Cieplak, C.I. Bayly, I.R. Gould, K.M. Merz, D.M. Ferguson, D.C. Spellmeyer, T. Fox, J.W. Caldwell, P.A. Kollman, A second generation force field for the simulation of proteins, nucleic acids, and organic molecules, J. Am. Chem. Soc. 117 (1995) 5179–5197.
[55] J. Wang, R.M. Wolf, J.W. Caldwell, P.A. Kollman, D.A. Case, Development and testing of a general amber force field, J. Comput. Chem. 25 (2004) 1157–1174.
[56] T. Lu, F. Chen, Multiwfn: a multifunctional wavefunction analyzer, J. Comput. Chem. 33 (2012) 580–592.
[57] E.G. Vega-Hissi, R. Tosso, R.D. Enriz, L.J. Gutierrez, Molecular insight into the interaction mechanisms of amino-2H-imidazole derivatives with BACE1 protease: a QM/MM and QTAIM study, Int. J. Quantum Chem. 115 (2015) 389–397.
[58] L.J. Gutierrez, E.E. Barrera, N. Peruchena, R.D. Enriz, A QM/MM study of the molecular recognition site of bapineuzumab toward the amyloid-β peptide isoforms, Mol. Simul. 42 (2016) 196–207.